



ADVANCED MASTERS IN STRUCTURAL ANALYSIS
OF MONUMENTS AND HISTORICAL CONSTRUCTIONS



Master's Thesis

Seyedeh Arezou Razavi Zadeh

Numerical modelling of bond in SRG-strengthened masonry

This Masters Course has been funded with support from the European Commission. This publication reflects the views only of the author, and the Commission cannot be held responsible for any use which may be made of the information contained therein.

DECLARATION

Name: Seyedeh Arezou

Email: Razavi zadeh

Title of the Msc Dissertation: Numerical modelling of bond in SRG strengthened masonry

Supervisor(s): Daniel V. Oliveira

Year: 2013

I hereby declare that all information in this document has been obtained and presented in accordance with academic rules and ethical conduct. I also declare that, as required by these rules and conduct, I have fully cited and referenced all material and results that are not original to this work.

I hereby declare that the MSc Consortium responsible for the Advanced Masters in Structural Analysis of Monuments and Historical Constructions is allowed to store and make available electronically the present MSc Dissertation.

University: Universidade do Minho

Date: July 16, 2013

Signature: _____

ACKNOWLEDGEMENTS

I would like to express my sincere appreciation to all the people who supported me throughout my thesis program. It has been an honour for me to work under the guidance of Professor Daniel Oliveira, whose continuous advice and support were very important in the completion of this research; hence, I express my profound sense of gratitude to him. I would also like to thank Mr. Bahman Ghiassi who not only kindly provided the experimental data used in this paper but also was a great help for all my technical and nontechnical problems. I heartily convey my sense of gratitude to him together with best wishes for his near future Ph.D. defence.

I greatly appreciate the facilities and supports provided by University of Minho that made it possible to carry on working in any situation and at any time. I thank Professor Lourenço and Professor Roca as coordinators whose great efforts in making this master course even better is much thankworthy. I also express my sense of gratitude to all other professors from each of the universities of SAHC who truly did their best during the coursework at Polytechnic University of Catalonia.

Being a part of the SAHC, I am really grateful to the European Union for both considering me as eligible to participate in this advanced masters course and providing the generous financial support through the Erasmus Mundus Scholarship.

The great moments I had during this master course have been definitely possible by having such great friends from all over the world. I thank them for making this year of my life as an unforgettable one. I would also like to thank my dear friend, Mahsa, whose encouragements and supports even from far distances made me more confident and blessed. I am also thankful to all my cousins who are my true friends especially Mahsa, Maryam, and Sara.

This acknowledgement would not be complete without expressing my sincere gratitude to my parents, for all the inspiration, reliance, and support they have given me throughout the course of my studies. I wholeheartedly thank my father for being a great source of inspiration and motivation in my professional life.

ABSTRACT

Regarding recent developments in the use of composite materials, they are being widely used as external strengthening systems. Among them Fibre Reinforced Polymers (FRPs) have shown successful applications even on masonry elements. However, considering some aspects such as sustainability and compatibility, they have shown deficiencies which have led to their being modified. As a matter of modification of FRPs, most recently mortar-based composites emerged. In case of special situations together with cutting on expenses, fibres have been also replaced by steel cords. Having a new composite strengthening system as steel reinforced grout (SRG), not only many problems regarding FRPs have been solved but also many benefits have been added. As a result, application of SRG strengthening technique has become more and more appealing in the field of strengthening and rehabilitation of structures particularly for upgrading the masonry elements.

Meanwhile, the effectiveness of the SRG strengthening system has turned out to be intrinsically dependent on the bond performance between the composite layer and the masonry substrate. As bond is a key mechanism in transferring stresses between the structural element and the composite material, a comprehensive understanding of its governing mechanisms is crucial for design and strengthening purposes. Thanks to the development of reliable numerical methods, now it is possible to investigate the required aspects with much less expenses as time and money.

The numerical model developed in this paper considers in detail characteristics of all the constituents, most noticeably the interfaces. Being able to justify the local bond stress-slip laws of the interfaces which play the role of the nonlinear behaviour in the system, this model is capable of reproducing different failure modes observed in real cases, i.e. the reference experimental works. A parametric analysis has been carried out by the proposed numerical model and results have been presented and discussed.

RESUMO

Os materiais compostos estão a ser largamente utilizados como sistemas de reforço externo de estruturas. Entre eles, os polímeros reforçados com fibra (FRP) têm sido aplicados com sucesso, mesmo em elementos de alvenaria. No entanto, considerando alguns aspectos como a sustentabilidade e compatibilidade, estes materiais mostraram algumas deficiências que têm conduzido a algumas modificações no seu uso. Deste modo, têm surgido recentemente materiais compósitos com matriz à base de argamassa, em que as fibras também têm sido substituídos por elementos de aço. Este novo sistema de reforço composto por aço reforçado com argamassa (SRG), resolveu alguns dos problemas relacionados com FRP's e trouxe também consigo novas vantagens. Como resultado, a aplicação da técnica de reforço SRG tornou-se atraente na área do reforço e reabilitação de estruturas, especialmente em elementos de alvenaria.

A eficácia do sistema de reforço SRG é intrinsecamente dependente do desempenho da ligação entre o material compósito e o substrato de alvenaria. Como a aderência é um mecanismo fundamental na transferência de tensões entre o elemento estrutural e o material compósito, é fundamental uma compreensão abrangente dos seus mecanismos para fins de projeto e reforço. Graças ao desenvolvimento de métodos numéricos fiáveis, é atualmente possível investigar numericamente os aspectos relacionados com a aderência com muito menos custos computacionais e temporais.

TABLE OF CONTENTS

1. Introduction.....	1
1.1. Strengthening and rehabilitation of structures	1
1.2. SRP and SRG as new strengthening techniques	2
1.3. Motivation and objectives of the research	4
1.4. Outline of the thesis	5
2. Literature survey.....	7
2.1. Recently developed techniques of strengthening	7
2.1.1. Use of FRP composites as a successful strengthening method	7
2.1.2. SRG composites compensating disadvantages of FRPs	8
2.2. Investigating the efficiency of SRG strengthening technique (experimental proofs) .	9
2.2.1. Application of SRGs on concrete members	9
2.2.2. Application of SRGs on masonry members	10
2.3. Bond resistance.....	12
2.4. Method of analysis of masonry elements	14
3. Available data from experiments at UMinho.....	17
3.1. Brief description of experimental procedure	17
3.2. Properties of materials.....	18
3.2.1. Bricks	18
3.2.2. Steel cords	19
3.2.3. Cementitious grout.....	19
3.3. Test set-up	20
3.4. Failure mechanisms and test results.....	21
3.4.1. Results of the experiments on the specimens of category 1	22
3.4.2. Results of the experiments on the specimens of category 2	22
3.4.3. Results of the experiments on the specimens of category 3	23
4. Numerical modelling.....	25
4.1. Constitutive laws of the materials.....	26
4.1.1. Brick, mortar, and steel cords	26
4.1.2. Steel-mortar interface	26
4.1.3. Brick-mortar interface	27
4.2. FE model	28
4.3. Calibration of the numerical model.....	29
4.3.1. SM bond stress-slip law sensitivity analysis-category 1	29
4.3.1.1. Elastic stiffness.....	29

4.3.1.2.	Maximum bond (shear) stress.....	30
4.3.1.3.	Residual bond stress	31
4.3.1.4.	Parameter S_1	31
4.3.2.	BM bond stress-slip law-category 1	33
4.3.3.	SM bond stress slip law -category 2.....	35
4.3.4.	BM bond stress slip law -category 3.....	36
4.4.	Verification of the model assumptions.....	37
5.	Parametric analysis	41
5.1.	Width of steel sheets.....	41
5.2.	Bonded length.....	43
5.3.	Thickness of the grout layer	44
5.4.	Parameters causing different failure mechanisms to happen	46
5.4.1.	Slippage of the steel cords (SM interface failure)	47
5.4.2.	De-cohesion of the grout from the brick (BM interface failure).....	47
5.4.3.	Tensile failure of the steel cords	50
6.	Conclusion and further remarks.....	53
6.1.	Main conclusions	53
6.2.	Remarks for further investigations.....	55
References	57

List of Figures

Figure 1 – Using twisted steel filaments in order to increase the interfacial shear strength and stiffness (Huang et al., 2005)	3
Figure 2 – Sample of steel cords and knitted yarns forming a net (Valluzzi, et al., 2012)	3
Figure 3 - A masonry SRG reinforced panel (Borri, et al., 2007).	3
Figure 4 - Construction of a SRG strengthened masonry arch (Borri, et al., 2007).	3
Figure 5 - Analytical bond stress-slip relationship (monotonic loading of reinforced concrete) (fib Bulletin No.55, 2010)	14
Figure 6 - Geometry of SRG strengthened brick specimens.	18
Figure 7 - Surfaces of the two types of bricks, left: original brick, right: sandblasted brick	18
Figure 8 – The steel cord consisted of twisted filaments used for the experiments	19
Figure 9 - Test set-up used at University of Minho	20
Figure 10 - Plates glued to the loaded end of the reinforcing steel strips for the loading to be transmitted uniformly.....	21
Figure 11 - Samples with original brick surface- de-cohesion of mortar from the brick.	21
Figure 12 - Samples with sandblasted brick surface- slippage of the steel cords from the mortar.	21
Figure 13 - Experimental results for the first category of specimens	22
Figure 14 – Experimental results for the second category of specimens.	23
Figure 15 – Experimental results for the third category of specimens.	24
Figure 16 - Local bond stress-slip relationship for SM interface.	27
Figure 17 - Local bond stress-slip relationship for BM interface.	28
Figure 18 - Finite element model.....	29
Figure 19 - Bond stress-slip law obtained based on the formulas of (CNR-DT200, 2012)	34
Figure 20 - The numerical model analysed with the adopted BM interface constitutive law. .	35
Figure 21 - Results of the parametric analysis on the number of steel cords.....	42
Figure 22 - Results of the parametric analysis on the bond length.	43
Figure 23 - Results of the parametric analysis on the thickness of the grout.	44
Figure 24 - Location of the nodes whose relative displacement indicated the slip of the model.....	46
Figure 25 - Normal stresses in steel cords in different load steps.....	50
Figure 26 - Tensile failure of different types of steel cords in different load steps.....	51

List of Tables

Table 1 - Mechanical properties of the brick elements.	18
Table 2 - Characteristics of the steel cords	19
Table 3 - Mechanical properties of the grout.	20
Table 4 – Summary of the categories of the specimens.	20
Table 5 - Average of maximum values of force and the corresponding slip – First category.	22
Table 6 - Average of maximum values of force and the corresponding slip – Second category	23
Table 7 – Average of maximum values of force and the corresponding slip – Third category	24
Table 8 - sensitivity analysis on the variable of "elastic stiffness".	30
Table 9 - sensitivity analysis on the variable of "Maximum bond stress".	30
Table 10 - sensitivity analysis on the variable of "Residual bond stress".	31
Table 11 - sensitivity analysis on the variable of " S_1 ".	32
Table 12 - The calibrated bond stress-slip law - SM - C1	32
Table 13 - The calibrated bond stress-slip law - SM – C2	36
Table 14 - The calibrated bond stress-slip law - BM - C3	36
Table 15 - Comparison of the tensile stress (σ_t) and strength (f_t) of the material-C1	38
Table 16 - Comparison of the tensile stress (σ_t) and strength (f_t) of the material-C2	38
Table 17 - Comparison of the tensile stress (σ_t) and strength (f_t) of the material-C3	39
Table 18 - The parameter changed in the analysis and the corresponding results.	42
Table 19 - The parameter changed in the analysis and the result.	43
Table 20 - The parameter changed in the analysis and the result.	44
Table 21 - Stress contours of materials in models P4 and the original model.	45
Table 22 - Studying the effect of different bond stress-slip laws of BM interface on the global bond-slip behaviour.	48
Table 23 - Parameters assigned for each of the BM bond-slip law.	48
Table 24 - BM bond stress-slip law which results in the failure mode of de-cohesion of the mortar from the brick.	49
Table 25 - Values of stresses in steel cords and corresponding bond forces and slips.	51

Chapter 1

Introduction

1.1. Strengthening and rehabilitation of structures

The requirement to strengthen and rehabilitate the structures is emerged due to presence of several damage factors which can be accounted for as vulnerability of structures to the natural hazards, harsh environment, aging, construction defects and other human caused problems. Consequently, the subject of rehabilitation and specially strengthening of structures is to increase the load bearing capacity that has become of great concern particularly in the case of infrastructures.

There are several methods of strengthening named reinforcing overlays or jacketing with concrete or steel plates, shotcrete, using post tensioning steel tie rods, using externally bonded fibre reinforced polymers and so on (Covatariu, 2011). Among these methods which are common in upgrading both concrete and masonry structures, using FRP composites has attracted much attention. Firstly named as advanced polymer composites (APC), these materials consisted of high strength and stiffness fibres protected by a high-performance thermosetting polymer. FRPs have remarkable characteristics which mostly depend on the characteristics of the fibre and the quality of the fibre/matrix interface. Good chemical resistance, low water absorption, high tensile strength, and excellent stiffness are some of the beneficial properties of these materials. This combination of properties made advanced composites to be vastly utilized in construction industry in which it is generally referred to as fibre reinforced polymer (FRP) (Hollaway, 2010). Besides the advantages of FRP composites there are also some disadvantages which have been the subject of many researches to be solved.

1.2. SRP and SRG as new strengthening techniques

The main obstacles to a widespread use of FRPs remain and are associated to their relatively high cost and lack of confidence in long-term durability. A new innovation in the use of composites is substituting the fibres, which are mostly of material group of glass, carbon, aramid, and basalt, with high strength steel wires forming cords. Hereupon, there is a new type of polymer composite called as steel reinforced composite (SRP). SRPs are less expensive composites and are currently considered for numerous applications in civil engineering, such as bridge and building repair (Huang, et al., 2005). In addition to the privilege of cost, the inherent shear strength of steel cords can simplify problems concerning connections and anchorages (Borri, et al., 2011).

The other issue of insufficient long-term durability of FRP composites, which is mainly concerned by low fire-resistance of epoxy resins used to glue the fibres to the substrate, has been solved by substituting the epoxy resin from the strengthening composite. A composite consisting of steel wires and a cementitious grout forms a new technique of strengthening named as steel reinforced grout (SRG). SRG composites are similar to their SRP counterparts, except for the polymer resin that is replaced with a cementitious grout. The grout that was found most suitable for the impregnation of the steel cord is a polymer-modified cementitious grout combined with a corrosion inhibitor (Borri, et al., 2011). Typically, these composites consist of steel wires forming cords that are assembled into a fabric and embedded within a matrix. Performance of a composite material utilizing steel wires is controlled by the stress transfer between the wires and the matrix. A single high-strength wire may be deficient due to low interfacial shear strength and stiffness. This problem is solved by using twisted steel filaments forming the cord, as shown in Figure 1. The rough surface of the cord provides a mechanical interlock with the matrix resulting in a system suitable for structural applications. Unidirectional cords can be held in place by knit yarns forming an appropriate pattern of fabric. The yarns control the spacing of the cords and as a result, the 'net' behaves like a fabric that can be stretched or bent, without losing its integrity (Figure 2).

SRGs have been successfully used in upgrading different concrete and masonry structures. In case of masonry members, it has been claimed that SRG strengthening technique can perform considerably effective especially in increasing one or more of the following parameters: tensile capacity, shear capacity, flexural capacity, member stability, strength or stiffness or both. Some experiments regarding either masonry panels or arches have been undergone to show the characteristics and potential of the SRG reinforced masonry (see Figure 3 and Figure 4) (Borri, et al., 2007). It is also worth mentioning that SRGs have been considered as a predominant technique because of their substantial low impact applications in reversibility and durability.

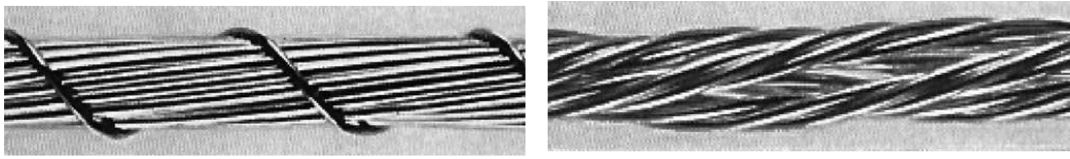


Figure 1 – Using twisted steel filaments in order to increase the interfacial shear strength and stiffness (Huang, et al., 2005)

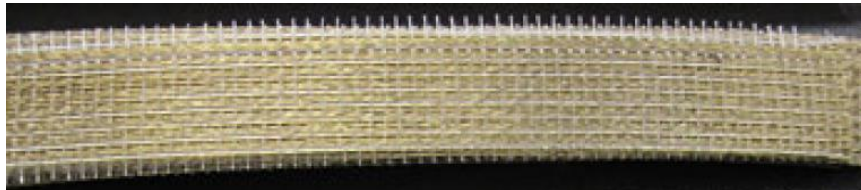


Figure 2 – Sample of steel cords and knitted yarns forming a net (Valluzzi, et al., 2012)



Figure 3 - A masonry SRG reinforced panel (Borri, et al., 2007).



Figure 4 - Construction of a SRG strengthened masonry arch (Borri, et al., 2007).

1.3. Motivation and objectives of the research

SRG strengthening method can be reliably used in practical applications only if their properties are known from experiments. Few existing studies on application of SRG strengthening technique prove its potentiality of improving the structural performance of both masonry and concrete elements (Wobbe, et al., 2004; Matana, et al., 2005; Huang, et al., 2005; Barton, et al., 2005; Borri, et al., 2009; Borri, et al., 2011). However, there is the lack of theoretical formulations regarding design purposes exclusively for SRGs on masonry substrates. It has been a common approach to adopt the formulas and laws included in standard documents and design guidelines for FRPs in order to estimate unknown parameters and data regarding SRG system (Grande, et al., 2013). Although close results may be obtained in this way it is evident that it is not based on reality and the influence of some aspects will be neglected or other irrelevant aspects will be considered. Knowing that there are fundamental differences between these upgrading systems, the need to develop theoretical models is totally justified. A comprehensive experimental work will result in vaster knowledge about behaviour of such techniques. Nevertheless, thanks to the development of numerical modelling techniques it is possible to lessen the amount of experimental tests and rely on powerful numerical methods.

Through this study the most important aspects influencing the performance of SRG strengthening technique will be investigated from the numerical point of view, namely the interaction mechanisms between different materials. As it is evident from present experimental works, the interaction of materials in the interfaces governs the failure mechanisms. By using the term “bond” that denotes the interaction and transfer of force between two different materials as the characteristic behaviour of interface zone, it has been tried to identify the effect of this phase on the global behaviour of the strengthened member. Accordingly, interface layers are defined in order to investigate the failure initiation, bond mechanisms, and other aspects in order to understand the behaviour more in detail. Hereupon, the main objectives of this dissertation are as follows:

- To develop a micro model representing a brick element strengthened with SRG under pull out test with the same conditions as the experimental work.
- To define local bond stress-slip laws for the two interfaces of steel-mortar and brick-mortar.
- To simulate the experimental results regarding global bond resistance-slip behaviour which is the key aspect in understanding the efficiency of this technique.
- To identify the effect of each interface characteristics separately on the global response of the system.
- To reproduce different failure modes observed in experiments from the numerical modelling.
- To carry out a parametric analysis in order to investigate the sensitivity of the method to different variable concerning geometry, material properties, etc..

1.4. Outline of the thesis

The organization of the content of this study considers 6 chapters covering different aspect relating to the subject. An introduction to the main points of the issue is brought in this first chapter.

The second chapter provides a survey on the state of the art in SRG strengthening technique. It comprises experimental and numerical studies as well as the applications of the method on masonry and concrete substrates. As the primary objective, the main focus was on the bond stress-slip laws of interface phase. Since the reference experimental work doesn't emerge any data on the state of the local behaviour of the interface phases, the similar conditions were investigated. For these approaches to define the local bond stress-slip relationships of the embedded reinforcement in reinforced concrete members have been discussed for this methodology. Later in this chapter the analysis method considered for the subject has been described.

Chapter three explains the experimental procedure in which material properties, test set up, and experiment's process are described. Material properties of the specimens are used directly in the numerical model. Test set up defines the boundary conditions in the numerical model and the test process specifies the simulation of applying the loads in the model. Drawing out the failure mechanisms observed from the experimental work, clarifies the main issues to be noticed later in the numerical simulation.

The numerical simulation is described in detail in chapter four. Starting from the basic concepts of numerical modelling, particularities of the model regarding defining different interface elements between different materials has been explained. Calibration of the bond stress-slip laws used to modify the interfaces and their consistency with analytical models is also discussed afterwards. Comparing the results obtained from the numerical model with the three categories of the experiments and seeing the good agreement between them, different failure modes are then shown. Finally, with the proposed model the state of the stresses in material has been checked to prove that the hypothesis about the behaviour of material is correct.

Chapter five is dedicated to the parametric analysis. The dependency of the strengthening technique to the change of variables regarding material properties, geometry of constituents, and other parameters has been investigated and described.

Finally, the overall conclusions and further remarks are presented in chapter 6.

Chapter 2

Literature survey

2.1. Recently developed techniques of strengthening

With the extant need for strengthening and rehabilitation of existing structures, several methods and techniques have been developed. Plesu et al. (PLEȘU, et al., 2011) have presented an overview of common methodologies for strengthening and rehabilitation of masonry structures using traditional materials. The techniques presented include repointing, injecting, and covering the cracks, adding wall buttresses, using reinforcing overlays (jacketing), the techniques of shotcrete, ferro-cement, and using seismic bands, reinforcing with external steel plates, bars, or post-tensioning tie-rods, using timber type wood elements, using pipes bracing system, reinforced concrete tie columns, and so on. None of the mentioned strengthening techniques presents such an advantage as to be preferred a priori to another; however each can be effective for specific masonry work or in the solution of a particular problem. On the other hand, newer technology options in this field are being developed from polymers, metals, ceramics and composites of these materials. Composites comprise of several different basic components that together provide physical characteristics superior to what each can provide separately. This old idea of composites has led to the relatively new technique of fibre reinforced polymers (FRPs) (Setunge, et al., 2002) which have become a popular material specially for external strengthening of masonry structures.

2.1.1. Use of FRP composites as a successful strengthening method

Early in the history of FRPs, they were first used in the constructions industry as a transparent material to radar or radio waves. During 1950s and into the 1960s the FRP material in building and in construction had a very chequered existence with inexperienced fabricators. It was in 1970s when

FRP composites were considered as a building material to design composite building structures. Constructions with FRPs by the mid-1980s were based on the properties of the composites as durability, high-strength and high stiffness which were particularly suitable for aggressive and hostile environments. These materials were also exploited in civil infrastructures. Early 1990s was the time FRPs started to be used for rehabilitation purposes as for repairing, non-seismic strengthening, and seismic retrofitting. From then on FRPs have been widely used and at the same time improved in different aspects (Hollaway, 2010).

FRP materials are characterized by excellent tensile strength in the direction of the fibres and by negligible strength in the direction transverse to the fibres; this illustrates the anisotropic nature of these materials. FRP composites do not exhibit yielding, but instead are elastic up to failure and they are also characterized by low compressive properties. Their function usually consists in adsorbing tensile stress due to shear and flexural actions. Often, among the reachable advantages, are also the increase of the overall stiffness and ductility.

Without underlining the importance of a lower installation cost, the use of FRP composites possesses some advantages compared to traditional retrofitting methods; as an example, the disturbance of the occupants and the facilities are minimal and there is no loss of valuable space. In addition, from the structural point of view, the dynamic properties of the structure remain unchanging because there is no addition of weight that would lead to increases in seismic forces (Morbin, 2002).

In summary, this technique has been used widely in many different situations and its capability of improving the structural performance has been proved by several studies. Nonetheless, FRPs have few drawbacks as being considerably expensive as well as being vulnerable in case of fire exposure. Also, its long-term behaviour is not totally known and some strength loss in time should be considered. The disadvantages caused them to be substituted with other methods which would overcome the shortages of this system.

2.1.2. SRG composites compensating disadvantages of FRPs

Steel reinforced grout (SRG) strengthening systems have been recently introduced as an alternative solution to the traditional systems based on the use of FRP materials. SRGs are consisted of very high strength and stiffness steel cords embedded in a cementitious grout acting as both adherent and an extra coating for steel cords which will serve them to enhance their corrosion resistance. The steel cords used in this upgrading system behave linearly in terms of stress-strain curve up to the failure which is unlike in steel materials. Use of this system brings about some advantages, naming as: adding shear capacity as a result of inherent shear strength of steel cords which also simplifies problems concerning connections and anchorages in addition to overcoming fire endurance and physical and chemical compatibility problems by using mortar matrix instead of epoxy matrix (Grande, et al., 2013). The performance of this strengthening system has been investigated in several studies which will be discussed in detail in the following sections.

2.2. Investigating the efficiency of SRG strengthening technique (experimental proofs)

2.2.1. Application of SRGs on concrete members

Huang et al. (Huang, et al., 2005) as a part in their study introduced steel reinforced grout-SRG composites. The performance of this strengthening technique is studied by them on the laboratory-prepared large-scale reinforced concrete beams. According to them, the stiffness and strength of the composites utilizing the steel cords differ due to a different cord surface geometry. That is different configurations of steel wires in a strand changes the surface roughness distribution which leads to different levels of stiffness and strength of the whole composite. Another aspect being studied was the issue of bonding between SRG and the parent material. In order to have a good cohesion the adhesive must be able to protect the integrity of the bond subjected to environmental and mechanical loads. For this reason, they got benefit from presence of other materials such as penetrating corrosion inhibitor in the impregnating grout to enhance some properties other than better adhesion to the substrate and gaining higher flexural and compressive strength. Additional freeze-thaw durability, more resistance to de-icing salts, and compatibility with thermal expansion coefficient of substrate, non-flammability, and non-toxicity are further advantages of the added corrosion inhibitor. They concluded that SRG can be easily and economically manufactured offering great potentials for strengthening through its easy and reliable bonding process. Finally, it was recommended that SRG can be successfully used for repairs and retrofit of the built infrastructure and even potentially in new constructions.

Through another study, (Matana, et al., 2005), the technology of SRG for structural retrofitting as a complementary technique of FRP has been evaluated by an experimental work aiming at evaluating the bond between SRG and the concrete substrate. They studied the influence of variables as type of reinforcement, surface roughness of the substrate, and bonded length in the direct shear test. Their results showed that SRG specimens experienced failure in the grout layer, leading to the conclusion that for these material systems a high level of concrete surface preparation may be required.

Barton et al. characterized reinforced concrete beams strengthened by steel reinforced grout (SRG) composites as part of their study (Barton, et al., 2005). Among the potentialities of increasing flexural, compressive, and shear capacities of reinforced concrete members by this strengthening technique, the flexural performance of RC beams with externally bonded SRG has been investigated experimentally using four-point bending test set-up in this paper. This study also considers this method of strengthening as a low-cost one which is consisted of high strength steel cords embedded in a cementitious grout being able to be applied using a wet lay-up technique similar to that of carbon or glass fibre reinforced polymer (FRP). About the characteristics of the internal reinforcing steel, it was said that its plasticity affects the laminate extensional, coupling, and bending stiffness. The final

results of this study were to develop the effective test methods to determine the material properties of SRG lamina. The reliability of the results was achieved by comparing them with the analytical ones.

Another study regards investigating the flexural capacity of reinforced beams externally bonded with SRP and SRG (Wobbe, et al., 2004). Wobbe et al. carried out an experimental work consisting of three specimens tested under four-point bending with variables considered including the number of reinforcement plies and types of bonding agents. Based on their test results, up to 100% increase in the flexural capacity can be achieved using these strengthening systems. In conclusion, their research program proved that this new technology has a great potential for the improvement of existing reinforced concrete structures.

Summing up the discussed researches, it is evident that the SRG strengthening technique is able to improve the structural performance of concrete elements in different aspects. The important issues to be regarded in this technique are the bond between the composite layer and the substrate as well as the characteristic of the steel cords and the grout. The matter of bond can be improved by a better surface preparation of the substrate as well as choosing grouts with enhanced properties. The influencing characteristic of the steel cords has been defined to be the arrangement of the strands as they control the roughness distribution which brings a better interconnection to the grout.

This technique has been also used on masonry structures which will be discussed further.

2.2.2. Application of SRGs on masonry members

Borri et al. (Borri, et al., 2009) investigated the efficiency of the innovative strengthening techniques of SRG and SRP for masonry arches through an experimental work. Their main objective was to assess the potential of steel cords to provide a strengthening system alternative to traditional techniques and to FRP laminates. They had ten prototypes of brickwork arches strengthened by composite laminates which were tested under a monotonic vertical load applied at the quarter span. Several parameters, named the types of reinforcement (steel and carbon fibres), types of matrices (epoxy and cementitious grout), the location of the strengthening layer (intrados, extrados, and both), and the presence of anchorage system, had been chosen to vary for the experiments in order to investigate their influence on the behaviour of the masonry arch. The analysis of the results obtained showed that strength gains provided by steel cords were greater than those obtained using carbon fibres regardless of either the location of the strengthening layers or the type of the matrices. The attainment of increases of both strength and ultimate deflection of minimum 18% was the proof for this statement. It should be noted that this result has been obtained despite the fact that FRPs have higher mechanical properties. According to them particularly for the case of SRG, this method is more effective for the intrados strengthening of the brick arches and the cementitious grout well behaved in bonding the steel cords to the masonry substrate and provided an overall better performance in terms of ultimate load capacity than the epoxy resin. Concluding the investigation, they reported that the strength of the arches reinforced with steel cords enhanced significantly. Consequently, with regards to the increase of

strength observed through their experimental work together with having less installation and material costs, their claim about the efficiency of SRG strengthening system was evidenced (Borri, et al., 2009).

As another application of SRG strengthening system for masonry structure, Borri et al. (Borri, et al., 2011) investigated the shear behaviour of masonry panels strengthened by this system. Investigating the effectiveness of the method in shear upgrading of masonry structures, they performed diagonal compression tests on specimens comprising of un-reinforced masonry (URM) panels as control specimens as well as strengthened panels manufactured using two different types of mortar. Their experimental results pointed out a significant increase in shear strength and stiffness, with interesting implications for the practical utilization of the technique studied.

As a matter of finding out about the interaction between masonry and steel cords which controls the stress transfer to the substrate and thus efficiency of the system, they investigated the local shear stress-slip behaviour through adhesion tests (both direct shear tests and pull-off tests) on samples strengthened by SRG. The outcome of the direct shear test revealed that in almost all cases SRG specimens showed a failure in the overlay which implies incapability of the matrix in transferring the stresses to the reinforcement. In the case of pull-off tests also, all SRG specimens failed in the interface, concluding to the statement that the failure type of SRG specimens is an adhesion failure. However, comparing this method with the FRP jacketing and ferro-cement techniques, which are all utilized for similar purpose of structural shear upgrading, the superiority of the SRG strengthening technique becomes evident. Firstly, SRG strengthening method obviates the use of epoxy resin which is used in FRP jacketing method and has unsolved problems in terms of high temperature and long term behaviour and compatibility. Secondly, with the SRG strengthening technique, the original facing remains perfectly intact and its ability to transpire remains unaffected which is counteracting the ferro-cement method by which the masonry is confined between two thin reinforced concrete walls. Lower material and installation costs have been counted as another advantage of this system as well.

Knowing that SRG strengthening technique can be efficiently used for upgrading of structures especially in case of shear retrofitting of masonry elements, it is needed to improve the technical recommendations which are non-existent or still in development. For this purpose, researchers (Borri, et al., 2011) have made comparison between experimental results and the predictions obtained by existing analytical formulations. As their conclusion, even though the proposed formulations are not specifically introduced for SRG, they may represent a useful instrument to calculate the reinforcement and can be considered as a starting point for more in-depth analyses. Among the different formulations they used for the comparison study, they found out that the formula proposed by Tomazevic (Tomazevic, et al., 1993) has led to an acceptable difference between analytical and experimental results. The obtained values differ by less than 40% and, in almost all cases, the proposed approach leads to conservative values when comparing with the experimental results. They stated that until new approaches to predict the shear capacity are available, the formula proposed by

Tomazevic appears to be adequate for design purposes, showing how the same approach used for masonry reinforced with steel bars or FRP can be satisfactory used for SRG.

In continuation of developing more reliable analytical formulations, it is needed to have a comprehensive understanding on the performance this technique. In addition to the few discussed investigations, this chapter focuses on the most important issue of this composite system which is the bond behaviour. In-detailed studies are discussed in the following sections.

2.3. Bond resistance

Since SRGs are fairly new technologies, there are still a number of questions related to the use of such materials as an efficient strengthening system. The state of the local bond behaviour of material interfaces is one of these questions. The bond of externally applied reinforcement is of critical importance for the overall performance of the composite system, since it is by means of stress transfer between the substrate and the composite layer that the composite action is developed (De Lorenzis, et al., 2001).

Grande et al. (Grande, et al., 2013) have investigated both experimentally and numerically the bond behaviour of masonry elements strengthened with SRP and SRG. Their experimental investigation evidenced that SRP and SRG systems are generally characterized by different bond mechanisms as expected. They defined this difference of bond behaviour in the two methods in terms of different failure mechanisms observed. As stated, SRP shows a de-cohesion mechanism which generally involves the failure of the masonry material, similarly to FRP in terms of mechanism but different in terms of bond resistance. Differently, the de-cohesion of SRG systems is quite complex because it can occur due to different failure mechanisms, such as the failure of the adhesive material and the slippage of the fibres; however it does rarely involve the failure of the support material.

On the basis of this consideration, they developed their numerical model to investigate on the interaction mechanism between the SRP/SRG system and the support. Their proposed approach is to suggest simple formulations based on those contained in the available technical document (CNR-DT200, 2012). The adopted formulations of the guideline contain coefficients experimentally calibrated especially for the case of FRPs. Considering the fact that there are some important differences particularly in terms of the de-cohesion mechanism of FRP and SRP/SRG, they evaluated firstly the bond resistance of the strengthened system by introducing some assumptions on bond strength and stress distribution, and secondly, they derived approximate bond-slip laws which were implemented in their numerical model.

Throughout their approach for the case of SRG, they evaluated the bond strength (τ_0) as an average value of that calibrated on an analysed experimental data where similar bond mechanisms of SRGs applied on clay bricks emerged. In their case, in spite of emerging different de-cohesion mechanisms for SRG system, their analysed data had evidenced a low variability of the bond strength.

Considering further assumptions, they evaluated the bond resistance of the strengthening systems which were later used to derive the bond stress-slip law. However, their study considers only a unique bi-linear bond stress-slip law which is used for their numerical approach of studying the interaction mechanism between the strengthening composite and the masonry support. It is a matter of concern that the interaction between the composite layer and the masonry support can be divided in the two phases of interaction between the steel cords and the grout and the interaction between the grout (including the steel cords) and the brick. This consideration is basically according to the experimental evidences which are explained in the chapter 3 of this paper.

Regarding the knowledge conceived, it was tried to consider the aforementioned approach in the related part of this study. The results and discussions have been presented in chapter 4.

On the other hand, the feasibility of steel cords as a part of reinforcing phase for composite materials is also another issue of concern. The performance of this strengthening technique is controlled not only by the stress transfer from the grout to the masonry substrate but also by the conveyance of the stresses between the wires and the matrix. As a result, the high quality of the interfacial mechanical interlock between the cords and matrix is crucial for a successful use of SRG (Borri, et al., 2011).

The way the bond mechanism works in the steel-mortar interface is still missing for analysing of this strengthening technique. Therefore, it has been tried to gather some general clues from similar cases. One of the cases has been considered to be the interaction between the reinforcing steel bars and the concrete in the reinforced concrete members. In spite of some fundamental differences between these two situations such as dimensions, material characteristic, arrangement of the reinforcement, and so on, the concept of shear stress transfer between the two materials can be regarded as the same.

The similarity of bond interaction in the two cases of reinforced concrete members and steel reinforced grout can be demonstrated by the way by Model Code 2010 (fib Bulletin No.55, 2010) that has defined the interface characteristics for the reinforced concrete elements. In the code, as a matter of explaining the behaviour of embedded steel reinforcement, the term “bond” has been used to denote the interaction and transfer of force between reinforcement and concrete. Evidently, bond influences the performance of concrete structures in several ways in different stages. It is also statistically accepted that under well-defined conditions, there is an average ‘local bond’ versus ‘local slip’ relationship which can be defined according to Figure 5 for monotonic loading in the cases of pull-out and splitting failure.

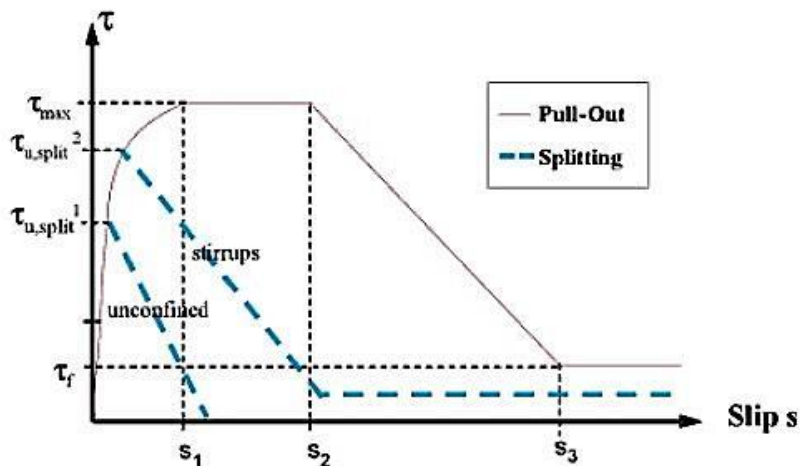


Figure 5 - Analytical bond stress-slip relationship (monotonic loading of reinforced concrete) (fib Bulletin No.55, 2010)

Among the three different relations shown in Figure 5, the one representing the bond stress-slip relationship for stirrups matches the case of embedded steel cords in the grout of the SRG system. This statement regards the facts firstly as the splitting failure type (this failure mechanism happens as a consequence of exceeding shear stresses) and secondly as the concept of resisting shear actions which occurs in both steel cords in SRGs and in stirrups in the reinforced concrete members.

After selecting the desired bond stress-slip relationship that illustrates the local bond-slip behaviour of the interface between the steel cords and the grout, it is important to obtain its parameters. The values of $\tau_{u,split}$, τ_f , s_1 , s_2 , and the rest has been defined in the model code for different bond conditions of the stirrups. Regarding missing some information, those parameters has been tried to be justified through a sensitivity analysis (described in detail in chapter 4). Moreover, further assumptions and conditions have been considered that will be presented as well.

The following section explains why the numerical approach has been selected to analyse and study the bond behaviour of the SRG strengthened masonry.

2.4. Method of analysis of masonry elements

As an alternative to experimental investigations, finite element (FE) models provide cost effective solutions in case of having the constitutive models for the material and the appropriate discretisation of the continuum. As a matter of analysing masonry elements which are of anisotropic material due to the presence of discrete sets of horizontal and vertical mortar joints and possess orthotropic strength and softening characteristics, it is needed to have not only the properties of masonry constituent materials but also their interaction reflecting the workmanship. Based on these considerations, micro and macro modelling techniques for the analysis of masonry have been provided (Dhanasekar, et al., 2008). In the macro analysis, masonry is considered as a single material (also known as homogenised

material) that inherently includes the effect of mortar joints. On the other hand, in the micro analysis, all constituents of masonry including the units and the mortar are separately discretised using continuum or discrete elements. Particularly within the numerical studies, the bond behaviour is usually modelled by using interface elements in a two or three dimensional space (Ghiassi, et al., 2012). Moreover, in a micro-model approach the effect of different parameters on the global performance and a more reliable stress distribution can be followed, which are the key issues in design procedures. Regarding the aforementioned facts as well as considering the scale of the model which is to be numerically simulated, the micro-modelling strategy has been considered in this study.

In order to find out the material constituents the reference data from the experimental work has been described in the following chapter.

Chapter 3

Available data from experiments

at UMinho

3.1. Brief description of experimental procedure

The experimental work whose results were the reference for the present study is described briefly. Single-lap shear bond tests have been performed at the University of Minho on specimens composed of a single brick as the masonry substrate with steel cords embedded in the cementitious grout applied on top as the strengthening component. It is worth mentioning that the direct shear test is widely used as an effective means for characterization of the bond between externally bonded reinforcement and the concrete (Chajes, et al., 1996), (De Lorenzis, et al., 2001).

The geometry of the specimens is illustrated in Figure 6. As it can be seen, steel cord strips of 50 mm width have been embedded in the 6 mm thick cementitious grout. The embedded length of the strips was equal to 150 mm with a 40 mm unbounded part at the loaded end. As for the specific conditions three different categories of tests were selected. 5 specimens with sandblasted brick surfaces which had been cured for 3 months constitute the category 1 and 3 samples consisting of the same type of bricks (with grinded surfaces) which had been cured for one month form the category 2 of the testing program. The category 3 comprises of 3 specimens whose brick surfaces were not sandblasted, as a result, had smooth surfaces. They also had been cured for one month. The tests were performed using a closed-loop servo-controlled testing machine under displacement controlled conditions. The displacements were imposed following a constant speed of 5 lm/ min at the end of the steel cord stirrups. The resulting load was measured by means of a load cell, while the slip of the steel cords had been measured.

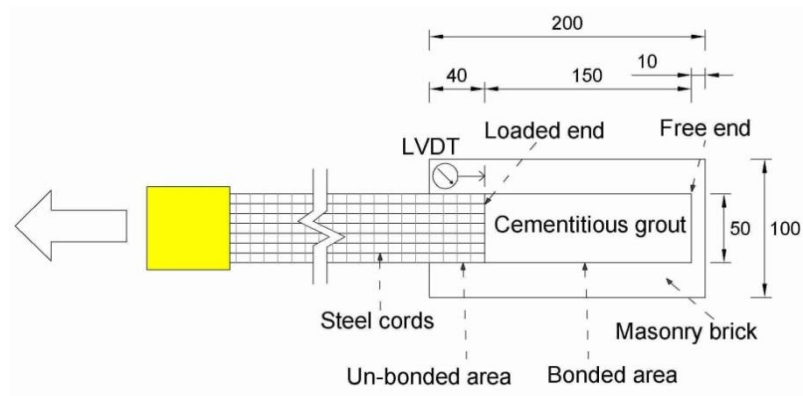


Figure 6 - Geometry of SRG strengthened brick specimens.

3.2. Properties of materials

3.2.1. Bricks

The masonry units used as the substrate were clay bricks with dimensions of $200 \times 100 \times 50 \text{ mm}^3$. As mentioned before, there were two types of bricks whose difference were in terms of the roughness of the front surface. For the first and second category of specimens the bricks had been sandblasted and for the third category original bricks with the smooth surfaces were used (see Figure 7). Table 1 presents the mechanical properties of the brick units in terms of elastic modulus and compressive strength.

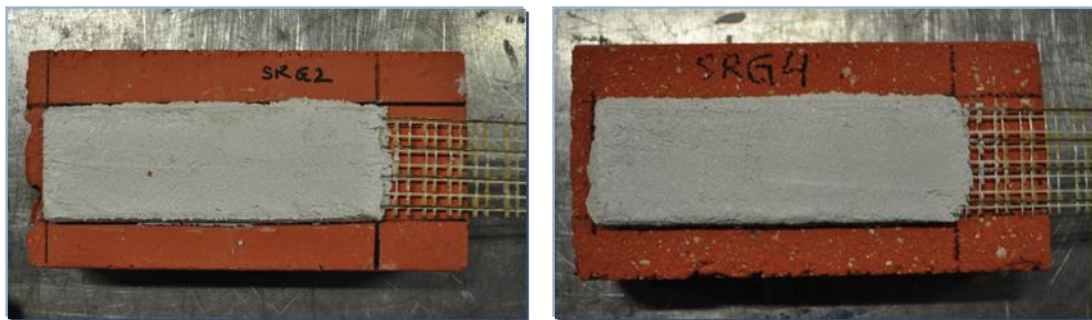


Figure 7 - Surfaces of the two types of bricks, left: original brick, right: sandblasted brick

Table 1 - Mechanical properties of the brick elements.

Elastic modulus [MPa]	9,500
Compressive strength [MPa]	14

3.2.2. Steel cords

In this strengthening system, unidirectional ultra-high tensile steel sheet (commercially referred to as FIDSTEEL 3X2-G 4-12-500 HARDWIRE™) was used. Each cord of the steel sheet is of high carbon steel with micro-fine zinc galvanized coating. The 3X2 cord is made by twisting 5 individual wire filaments together – 3 straight filaments wrapped by 2 filaments at a high twist angle resulting in the increase of the interfacial shear strength and stiffness of the steel-mortar interface (Figure 8). The cords are held in place by using knit yarns which form an appropriated pattern of the fabric with fixed spacing and integrity.

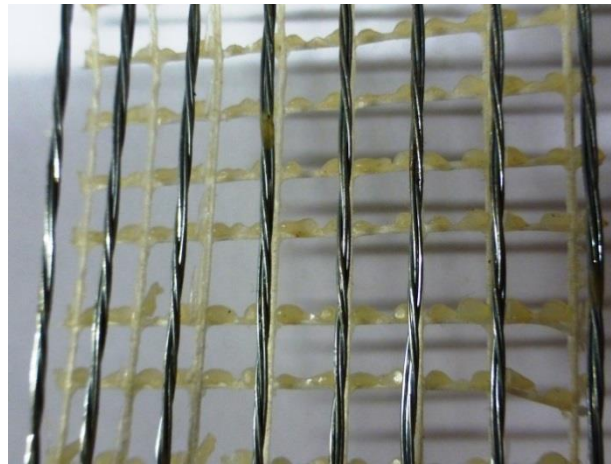


Figure 8 – The steel cord consisted of twisted filaments used for the experiments

Characteristics of the steel cords have been summarized in Table 2.

Table 2 - Characteristics of the steel cords

Elastic modulus [MPa]	190,000
Tensile strength [MPa]	2820
No. of cords	8
Cross section of each cord [mm ²]	0.538

3.2.3. Cementitious grout

In order to see the effect of the mechanical properties of the grout on the properties of the interfaces two types of cementitious grout were prepared. The one cured for one month was used for test specimens of category 2 and 3 and the three-month cured grout was applied for the first category of the specimens. Mechanical properties of the grout are presented in Table 3.

Table 4 summarizes the categories of specimens being tested in the experimental procedure.

Table 3 - Mechanical properties of the grout.

Elastic modulus (measured from 3-month cured specimens) [MPa]	14,000
Compressive strength (1-month cured specimens) [MPa]	12.6
Compressive strength (3-month cured specimens) [MPa]	13.3

Table 4 – Summary of the categories of the specimens.

Specimen	Brick surface treatment	Mortar age at testing
Category 1	Sandblast	3 months
Category 2	Sandblast	1 month
Category 3	Original surface	1 month

3.3. Test set-up

The measurement system consisted of a linear transducer placed at the loaded end of the composite. The data recorded by this LVDT was the displacement of the steel cords relative to the brick support. The test apparatus at the University of Minho is designed and built allowing easy use of the available universal testing machine. Figure 9 shows the picture and the scheme of the test set-up. The steel device used was designed to be fixed to already available rigid steel testing frames, and the reinforcement was loaded from above. The specimen was positioned on the steel device and firmly clamped to it. In order to apply the load, the loaded end of the composite strip was glued between two plates to be confident that the transmission of load in the clamped area is uniform (Figure 10).

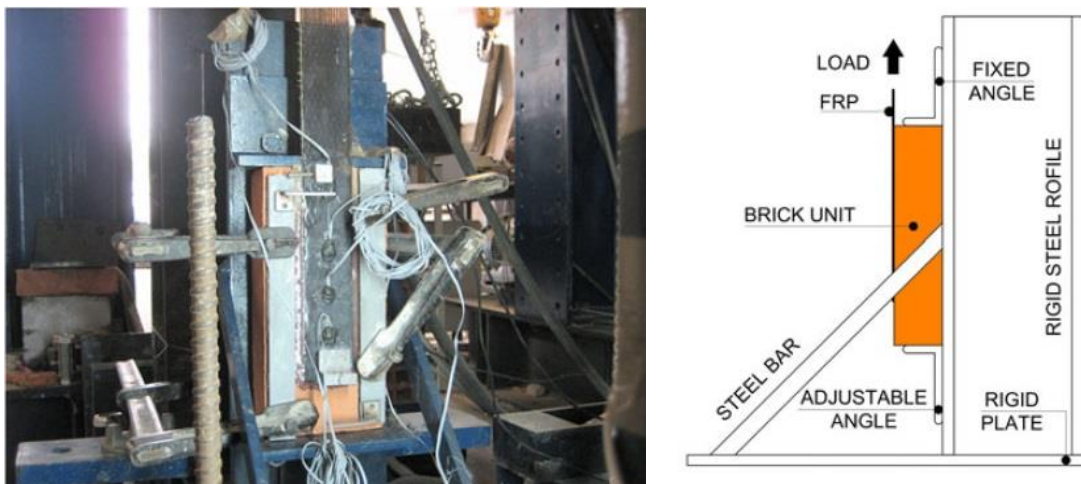


Figure 9 - Test set-up used at University of Minho

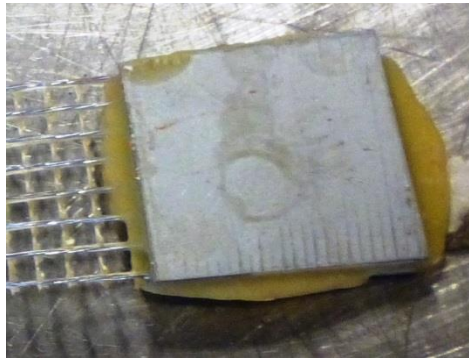


Figure 10 - Plates glued to the loaded end of the reinforcing steel strips for the loading to be transmitted uniformly.

3.4. Failure mechanisms and test results

In general two different failure mechanisms were observed which was dependent on the type of the brick. The bricks with sandblasted surfaces led to slippage of the steel cords from the mortar (Category 1 and 2 of the specimens, see Figure 11 and Figure 12). And the bricks with smooth surfaces caused de-cohesion of the mortar from the brick to happen (Category 3 of the specimens, see Figure 11 and Figure 12). The results of the experiments are presented for each category of specimens.



Figure 11 - Samples with original brick surface- de-cohesion of mortar from the brick.



Figure 12 - Samples with sandblasted brick surface- slippage of the steel cords from the mortar.

3.4.1. Results of the experiments on the specimens of category 1

Category 1 of the experimental work consisted of 5 specimens which have been cured for three months. Additionally, surfaces of the bricks were sandblasted. The result of the direct shear test on these specimens is presented in Figure 13 showing the maximum and minimum envelop and the average values. The failure mechanism observed was the slippage of the cords from the mortar. This failure mode was expected as the rough surface of the sandblasted brick could provide sufficient interlock between the brick and the mortar which prevented the detachment between them. Maximum shear force resisted by the specimens together with the corresponding slip has been shown in Table 5.

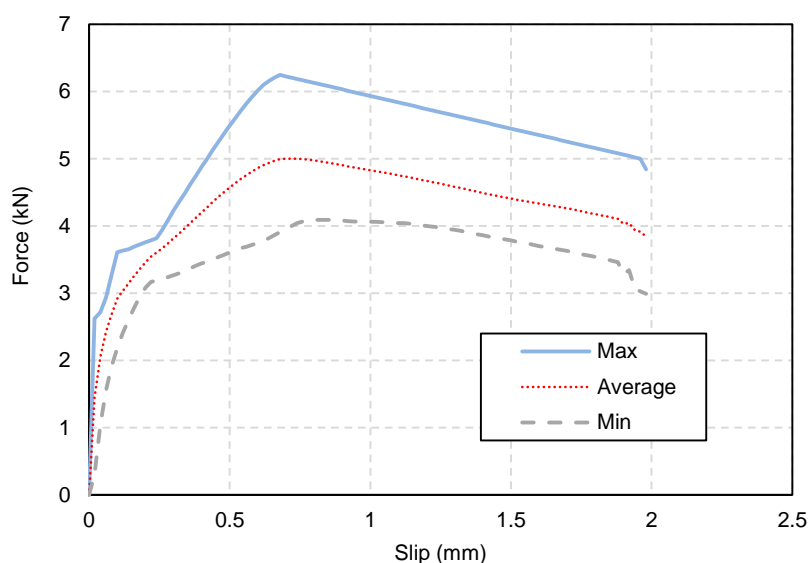


Figure 13 - Experimental results for the first category of specimens

Table 5 - Average of maximum values of force and the corresponding slip – First category

F_{\max} – average [kN]	5
Slip corresponding to F_{\max} – average [mm]	0.72

3.4.2. Results of the experiments on the specimens of category 2

In category 2 of the experimental work, 3 specimens which have been cured for one month were tested. Surfaces of the bricks in this case also were sandblasted. As expected, similar failure mode of slippage of the steel cords (as for the category 1 of specimens) was observed. Results are presented in Figure 14 and Table 6.

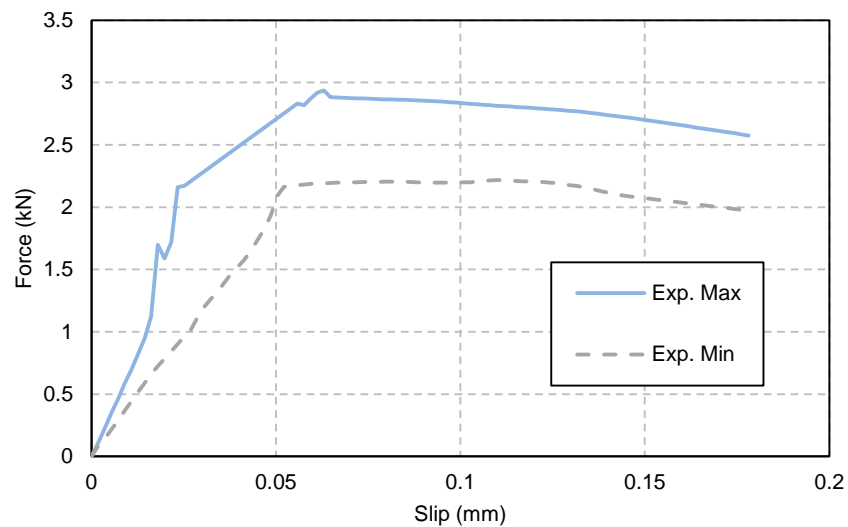


Figure 14 – Experimental results for the second category of specimens.

Table 6 - Average of maximum values of force and the corresponding slip – second category

F_{\max} – average [kN]	2.58
Slip corresponding to F_{\max} – average [mm]	0.072

3.4.3. Results of the experiments on the specimens of category 3

Category 3 of the specimens includes those 3 samples which were cured for one month and the surfaces of the bricks were completely smooth, as the original clay bricks were used. Results are presented in Figure 15 and Table 7. It should be noted that the peak load in this experiment refers to the maximum load the brick-mortar interface can resist since the failure mechanism observed was the detachment of the composite layer (the grout including the steel cords) from the brick.

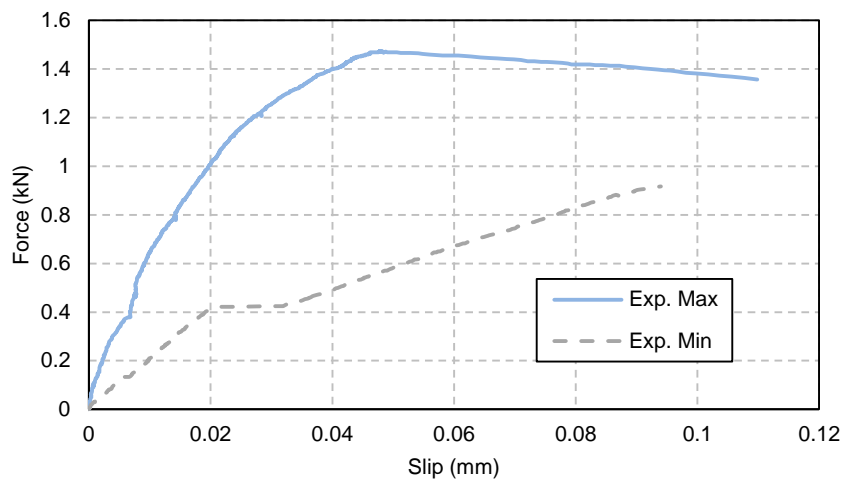


Figure 15 – Experimental results for the third category of specimens.

Table 7 – Average of maximum values of force and the corresponding slip – Third category

F_{\max} – average [kN]	1.2
Slip corresponding to F_{\max} – average [mm]	0.05

Regarding the results obtained in the three categories, it can be seen that different characteristics of specimens lead to different values for bond resistance and failure modes. Consequently, it is concluded that the final bond resistance of the system depends considerably on the characteristics of the specimens constituents.

Chapter 4

Numerical modelling of SRG

Numerical modelling of masonry structures can be done in several ways. Nevertheless, the most suitable method is dependent on the structure under analysis, the available input data and the analyst's experience and qualifications (Lourenço, 2002). In case that the best method is defined as the one providing the sought information in a reliable manner, i.e. within an acceptable error, the best method can be the one with the least cost (Oliveira, 2003). Detailed micro-modelling technique was chosen for the present case in which both unit and mortar are discretized and modelled with continuum elements whereas the unit-mortar interface is represented by discontinuum elements. Regarding the experimental test which is to be simulated and defines the size of the specimen and scale of the work, it is the best to use the analysis with this level of refinement. Hence, it is possible to carry out a detailed analysis of unique brick specimens strengthened with SRG. The micro-modelling strategy of masonry structures consists of modelling units with elastic continuum elements and joints with inelastic interface elements.

Contrary to (Grande, et al., 2013) who have used only one interface for SRG strengthened masonry elements, two different interfaces have been adopted for the present study. The first interface, named as BM, represents the joint between brick and mortar and the second interface is the representative of steel-mortar joint and is named as SM. The characteristics of both interfaces are important as they govern the failure mechanisms. A very weak BM interface, as the interface between bricks with smooth surfaces and mortar, leads to detachment of the mortar from the brick. Meanwhile, having a strong BM interface by sandblasting the surfaces of the bricks changes the failure mechanism to decohesion of the steel cords from the mortar. Later this phenomena occurs, higher will be the capacity of the strengthening system in increasing the shear resistance of the structure. This fact represents the role of the characteristics of the SM interface on the global behaviour of the system. The third failure mechanism, which is the tensile failure of the steel wires, is also influenced directly by the properties of its interface with the mortar.

According to the aforementioned failure mechanisms, damage is modelled as interfacial de-bonding in one of the two interface elements. However, defining an appropriate bond-slip law plays the important role for the model to be accurate. The bond-slip laws for the interface elements can be a function of the adhesion of the material to each other, bonded area, and mechanical properties of the components. This functionality is neither elaborated in the codes and strengthening guidelines nor can be obtained directly from the experiments. SRG strengthening technique as a new born method in the case of upgrading masonry elements lacks theoretical formulations in design codes and guidelines; nonetheless, in some cases formulas of FRP composites have been adopted in order to extract the bond stress-slip law for the interfaces (Grande, et al., 2013). Although sufficiently good results were obtained it doesn't fulfil the requirement for bond-slip formulations particularly for SRG system as the constitutive components are completely different from the FRPs. (Ghiassi, et al., 2012) have used the bond-slip law obtained directly from the results of shear bond tests, however, in this case it is not possible to measure the bond-slip characteristics of the strengthening component since the steel cords are embedded in the mortar. Therefore, the peculiarity of this study is the way the bond stress-slip law has been determined for the interfaces.

4.1. Constitutive laws of the materials

4.1.1. Brick, mortar, and steel cords

As discussed before, linear elastic behaviour is considered for the constitutive material, namely brick, mortar, and steel cords. These unites have been considered isotropic as well. The validity of this hypothesis will be discussed comprehensively afterwards.

4.1.2. Steel-mortar interface

In this study, only interfaces have nonlinear behaviour. According to the explanations of section 2.3 the constitutive law regarding the bond stress-slip relationship for the stirrups embedded in the reinforced concrete members (fib Bulletin No.55, 2010) have been adopted to define the bond stress-slip law of the embedded steel cords of the SRG system. Consequently, it can be said that for monotonic loading the bond stresses between grout and steel wires for sliding behaviour can be calculated as a function of the relative displacement s according to Equation 1, Equation 2, and Equation 3 (see Figure 16).

Equation 1

$$T = T_m (s/s_0) \quad \text{for} \quad 0 \leq s \leq s_0$$

Equation 2

$$T = T_m (T_m - T_r) (s - s_0) / (s_1 - s_0) \quad \text{for} \quad s_0 \leq s \leq s_1$$

Equation 3

$$T = T_f \quad \text{for} \quad s_1 \leq s \leq s_2$$

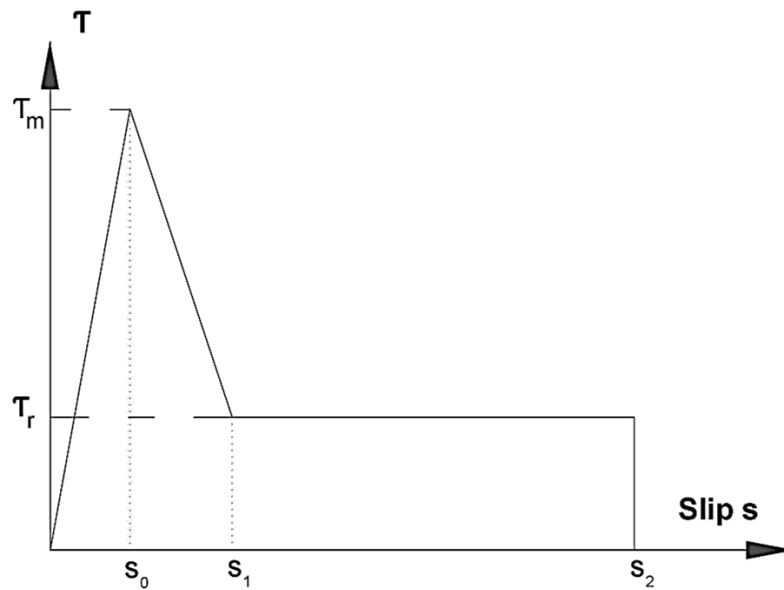


Figure 16 - Local bond stress-slip relationship for SM interface.

Where T_m (bond strength), T_r (residual bond stress), s_0 (slip corresponding to T_m), s_1 (slip at the end of softening branch where cohesion is lost and only friction resists the slip occurring afterwards), and s_2 (the ultimate slip) have been defined through calibration of the model with the experimental results. As a matter of justification, the shape of the graph has been selected in a way that complexities of pre-peak and post-peak branches are simplified to linear behaviour (i.e. the nonlinear branch between the elastic regime and the peak value has been omitted). Lack of experimental clues on local behaviour of the interface as well as the fact that the simplified model is representative of the behaviour observed in experimental results allows for consideration of such local behaviour. The simplified bond stress-slip law of the SM interface implies a first linear elastic behaviour as the pre-peak branch followed by a linear softening part representing loss of cohesion between the two materials in the interface. The third branch with the constant bond stress of T_r represents the frictional resistance of the interface.

4.1.3. Brick-mortar interface

BM interface is justified by the constitutive bond stress-slip law as indicated in Figure 17. Having a bilinear trend, it is similar to bond-slip laws introduced in CNR-DT200 for the design of externally bonded FRP systems for strengthening existing structures. Although the constituent material of the strengthening system differs from those considered for the guideline, it has been shown in another study (Grande, et al., 2013) that its application will result in reliable outcomes. However, the parameters have been calibrated in order to account for specifications of the experimental work which was to be simulated.

The following sections report the procedure of justification of the numerical model in terms of the calibration of the elastic stiffness, bond strength, ultimate slip, and so on for both SM and BM interfaces.

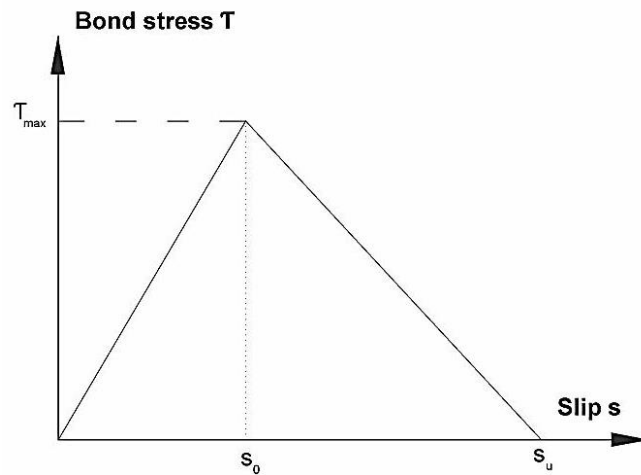


Figure 17 - Local bond stress-slip relationship for BM interface.

4.2. FE model

A plane stress finite element (FE) model in the FE code DIANA (DIANA, 2009) was used to simulate the experimental results obtained from the testing program described in chapter 3. The adopted mesh comprises eight-node plane stress elements (labelled as CQ16M in DIANA) in order to represent the brick and the grout element, two-node truss elements (labelled as L2TRU in DIANA) for steel cords, and two sets of six-node zero-thickness interface elements (labelled as CL12I in DIANA) for brick-mortar and steel-mortar interfaces. The constitutive laws of material described in the previous section have been adopted for this numerical analysis. The constraints and loading conditions were based, respectively, on the test set up and the incremental monotonic displacement load which is illustrated in Figure 18. Solving the nonlinear equations was on the basis of a modified Newton-Raphson iterative scheme together with the line search method.

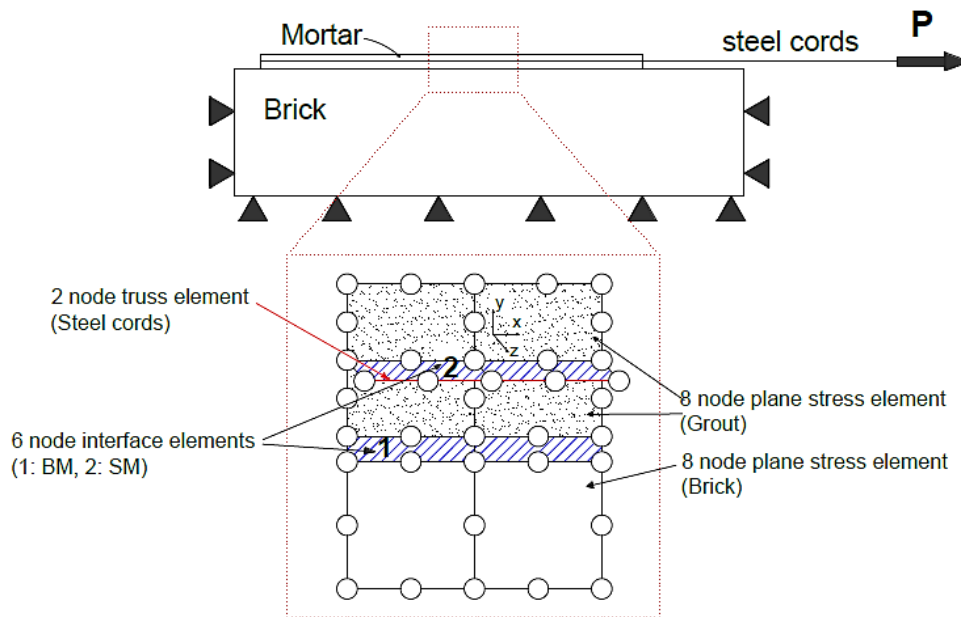


Figure 18 - Finite element model.

4.3. Calibration of the numerical model

4.3.1. SM bond stress-slip law sensitivity analysis-category 1

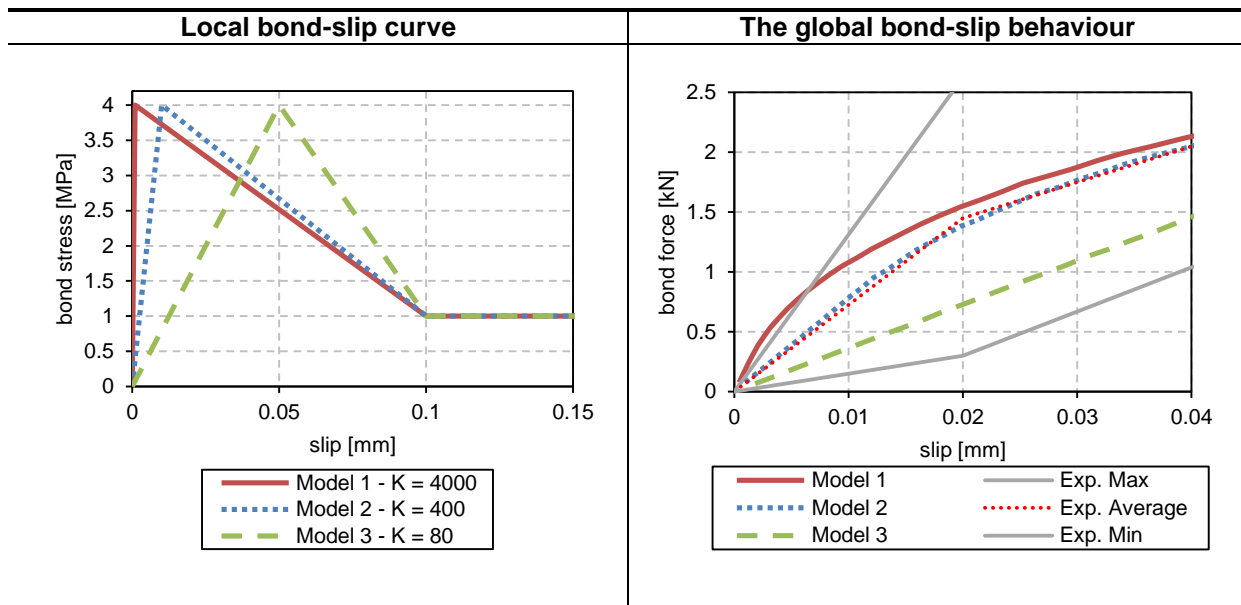
The parameters of the constitutive law introduced in section 4.1.2 were obtained through the sensitivity analysis. This analysis studies the effect of each variable on the global response of the model. The procedure which comes hereafter explains how the variables of the bond stress-slip law for the SM interface have been calibrated according to the experimental results of the first category of the specimens.

It should be noted that in order to be confident that only the failure mechanism observed in the corresponding experimental tests will occur, the bond stress-slip law for the BM interface was considered to be perfectly bonded. The fact that this hypothesis will interfere with the global behaviour of the model or not will be discussed in section 4.3.2.. In each of the following sections one variable of the constitutive law has been changed so as to understand the effect of that specific variable on the global response of the model.

4.3.1.1. Elastic stiffness

The three different bond stress-slip laws which have been assumed in this section have three different elastic stiffness values. K_1 (the shear stiffness in model 1) is equal to 4000, K_2 has been assumed as 400, and K_3 is 80 [N/mm³]. The rest of parameters as the bond strength, residual stress, and S_1 have been assumed as equal. The procedure has been presented in Table 8.

Table 8 - sensitivity analysis on the variable of "elastic stiffness".

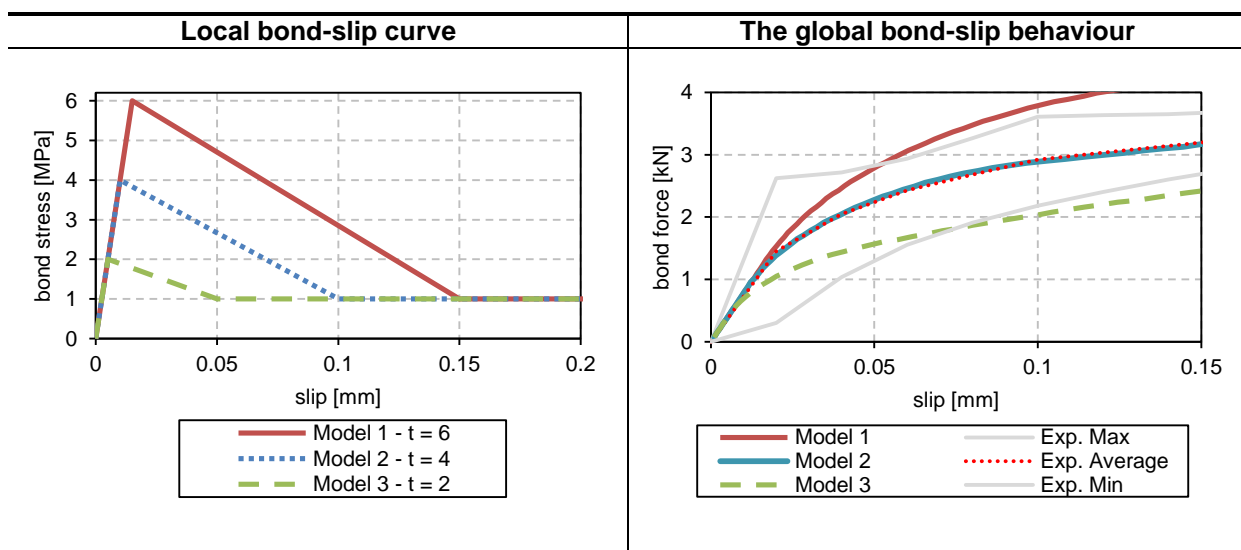


As it can be seen, the elastic stiffness of the bond stress-slip law, which is also referred to shear stiffness, has a direct influence on the resulting bond-slip behaviour of the model. Consequently, the optimum value of the shear stiffness can be considered around $400 \text{ [N/mm}^3\text{]}$ which seems to result in a global bond-slip behaviour with the same initial stiffness as the average of the experimental results.

4.3.1.2. Maximum bond (shear) stress

The three bond strengths considered in this study are: $\tau_{m1} = 6 \text{ [MPa]}$, $\tau_{m2} = 4 \text{ [MPa]}$, and $\tau_{m3} = 2 \text{ [MPa]}$. The corresponding bond-slip graphs have been shown in Table 9.

Table 9 - sensitivity analysis on the variable of "Maximum bond stress".

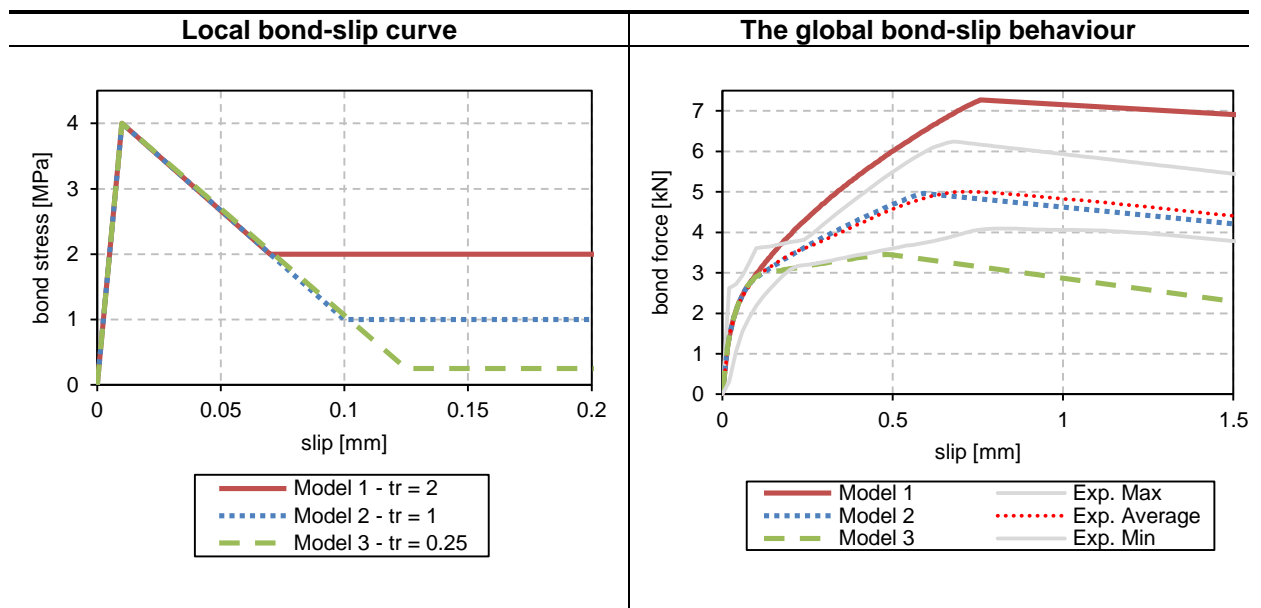


The direct influence of the value of the bond strength is also evident in the results. As it can be seen, higher bond strength in the bond stress-slip law of the interface results in a higher value of the bond resistance in the global bond-slip behaviour of the model. This study provides the value of the optimum bond strength to be around 4 [MPa].

4.3.1.3. Residual bond stress

The same procedure was taken in this section and three different values for T_r have been considered. T_{r1} , T_{r2} , and T_{r3} have been assumed to be 2, 1, and 0.25 [MPa], respectively. Table 10 illustrates the assumptions of the models together with the results.

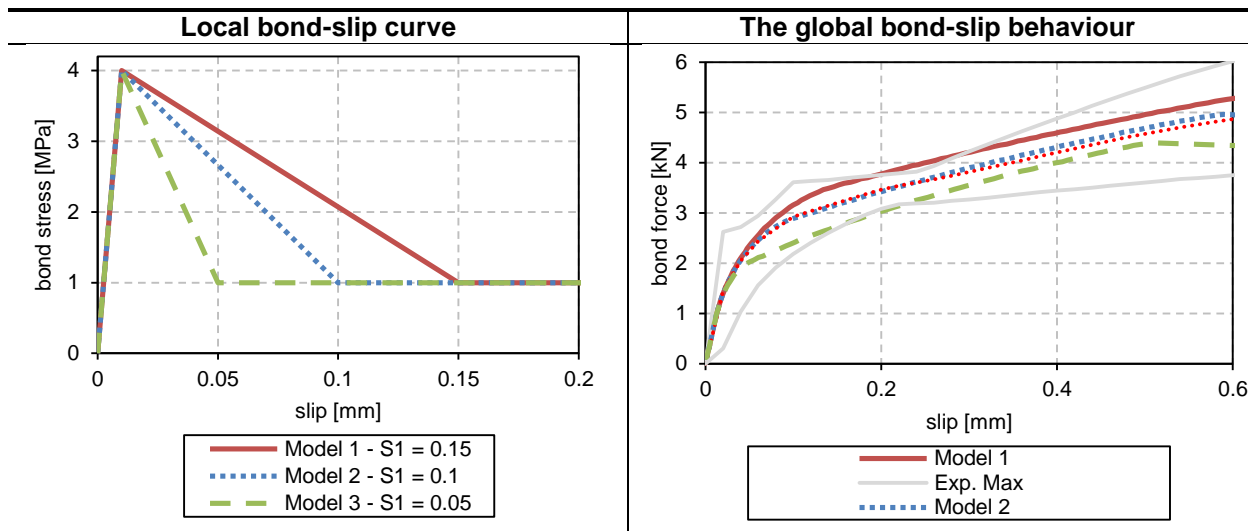
Table 10 - sensitivity analysis on the variable of "Residual bond stress".



It can be concluded from the graphs that the value of the residual bond influences the hardening branch of the global bond-slip behaviour significantly. Accordingly, the optimum value of T_r can be in the range of 1 [MPa].

4.3.1.4. Parameter S_1

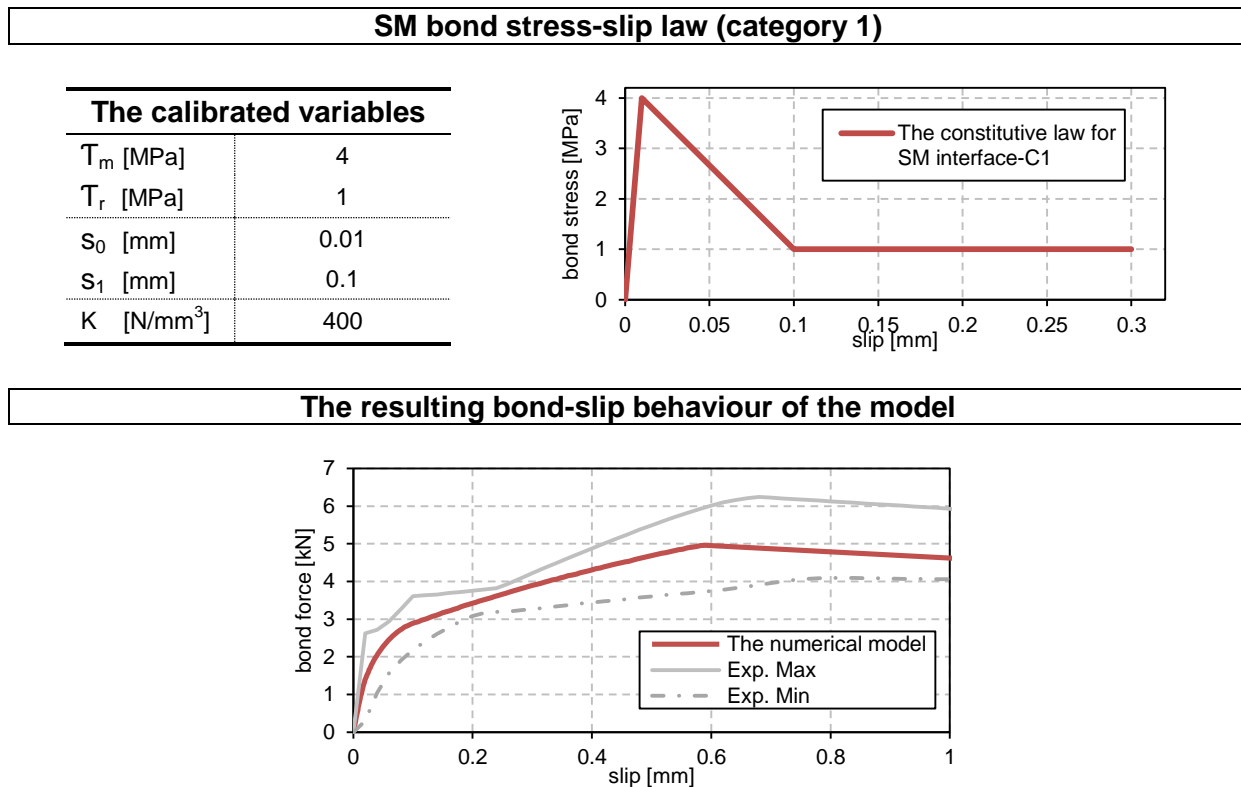
S_1 is the slip value in the bond stress-slip law of the interface which corresponds to the point of the beginning of the residual strength. Assuming three different values for this parameter, its effect on the global bond-slip behaviour has been studied. Table 11 summarizes the assumptions and the results of this analysis.

Table 11 - sensitivity analysis on the variable of " S_1 "

Regarding the results obtained, it becomes clear that the effect of the parameter S_1 in the local bond stress-slip law is on the value of the elastic bond limit of the global bond-slip behaviour. The relationship is direct and the best value for S_1 can be considered as 0.1 MPa.

Summing up all the results obtained through the sensitivity analysis, it can be concluded that the constitutive bond stress-slip law for the SM interface in case of simulating the category 1 of the experimental tests described in chapter 3, will have the parameters as indicated in Table 12.

Table 12 - The calibrated bond stress-slip law - SM - C1



4.3.2. BM bond stress-slip law-category 1

As discussed before in chapter 2, Grande et al. have introduced a bond stress-slip law for the interface between the strengthening composite and the masonry substrate in the SRG strengthening technique in their proposed numerical model (Grande, et al., 2013). This law was adopted from CNR-DT200 (Guide for the design and construction of externally bonded FRP systems for strengthening existing structures). As it was perceived they had considered an equivalent steel sheet as the reinforcing phase and the grout would be the adhesive phase which is close to the overall arrangement of FRP or SRP composites. With this assumption, the formulas of that guideline could be used. This assumption neglects the two different interfacial behaviours of steel-mortar interface and brick-mortar interface which is actually important to be considered as it leads to having different failure mechanisms. Nonetheless, their model worked sufficiently good to simulate their experimental results.

In this section that the BM interface properties are being dealt with, it was tried to adopt similar bond stress-slip law as it is considered in the aforementioned paper. The validity of this assumption is based on the fact that they have considered the failures modes either as interfacial failure or the failure of the mortar. Since the governing failure mode which helps to characterize the properties of the bond stress-slip law of the BM interface is close to this assumption, this hypothesis can be assumed to be valid.

The following procedure explains how the parameters of the constitutive law for BM interface have been calculated.

The value of T_{max} as the bond strength was considered to be 1 MPa in order to have an approximate value since there are no experimental measurements for it (this value was assigned as 1.8 MPa in the work of Grande et al., based on the average of their experimental results). Having the bond strength and calculating the elastic stiffness of the law from Equation 4, it will be possible to obtain the value of S_0 from the Equation 5.

Equation 4 – Elastic shear stiffness of the bond stress-slip law for the BM interface.

$$G_e = \frac{1}{\frac{t_a}{G_a} + \frac{t_m}{G_m}}$$

Equation 5 - Slip corresponding to the maximum bond stress.

$$S_0 = \frac{\tau_m}{G_e}$$

Where in Equation 4, G_e is the elastic stiffness which is in fact the shear modulus of the interface, $t_a(G_a)$ and $t_m(G_m)$ are the thickness (shear modulus) of the adhesive and the masonry, respectively.

Putting the appropriate values in these equations, the results below will be obtained:

$$G_e = \frac{1}{\frac{3}{5.83} + \frac{50}{3.96}} = 76 \left[\frac{MPa}{mm} \right]$$

Resulting to have the value of S_0 as:

$$S_0 = \frac{1}{76} = 0.013 \text{ mm}$$

In order to obtain the remaining parameters of the bond-slip law, fracture energy has been calculated through Equation 6.

Equation 6 - Evaluating the fracture energy.

$$\Gamma_f = \frac{F_{max}^2}{2 \cdot b_f^2} \left(\frac{1}{E_f \cdot t_f} + \frac{b_f}{E_m \cdot t_m \cdot b_m} \right)$$

Where F_{max} is the bond resistance of the SRG strengthening systems which can be assigned as 5 kN from the average value of the experimental results, E_f (t_f) (b_f) and E_m (t_m) (b_m) are the elastic stiffness (thickness) (width) of the reinforcement and the masonry, respectively. Therefore, the value of fracture energy will come out as:

$$\Gamma_f = \frac{5000^2}{2 \times 50^2} \left(\frac{1}{190E3 \cdot 0.084} + \frac{50}{9.5E3 \cdot 50 \cdot 100} \right) = 0.318 \left[\frac{N}{mm} \right]$$

Now, the ultimate slip, S_u can be calculated from Equation 7.

Equation 7 - Ultimate slip value of bond stress-slip law.

$$S_u = 2 \cdot \frac{\Gamma_f}{\tau_m} = 2 \cdot \frac{0.318}{1} = 0.637 \text{ [mm]}$$

The resulting bond stress-slip law will be as it is shown in Figure 19.

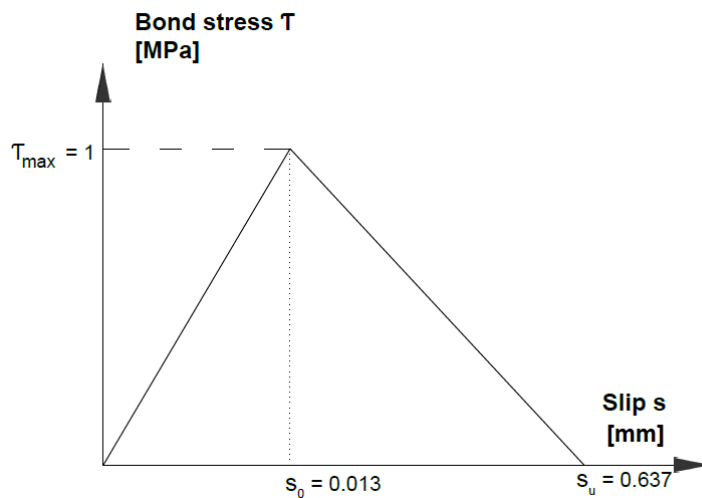


Figure 19 - Bond stress-slip law obtained based on the formulas of (CNR-DT200, 2012).

The bond stress-slip law obtained has been put in the numerical model instead of the perfectly bonded BM interface and the updated result came out as it is shown in Figure 20.

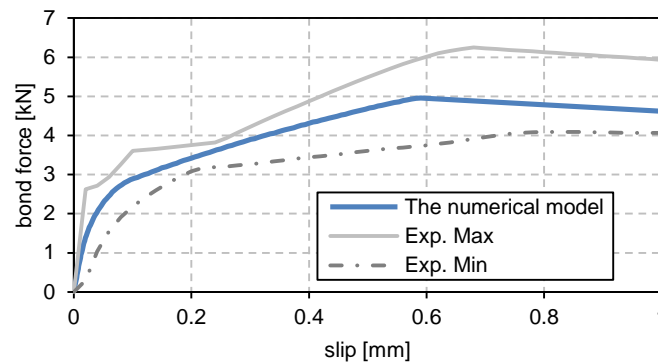


Figure 20 - The numerical model analysed with the adopted BM interface constitutive law.

Although this method of calculating the bond stress-slip law for the BM interface is not completely based on the real situation and comprises some simplifications and approximations, it provided a good approach to know that even considering this law will lead to the same results as assuming a perfect bond BM interface. Therefore, it is possible to say that in case of category 1 specimens and in case of not having any information about characteristics of BM interface it can be assumed as a perfectly bonded interface. It should be noted that the observed failure mechanism should correspond to this assumption. In other words, in the case studied in this section the only failure mechanism observed was the slippage of the steel cords from the mortar and not de-cohesion of the mortar from the brick. Otherwise, this assumption should be revised.

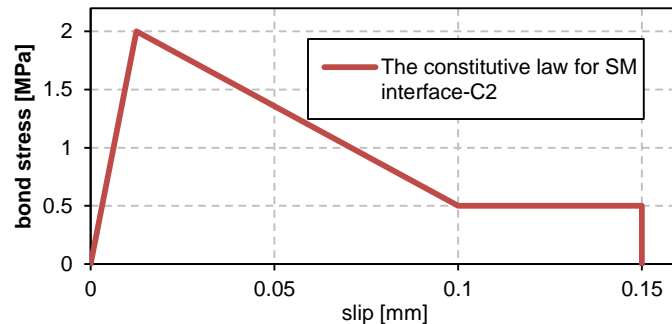
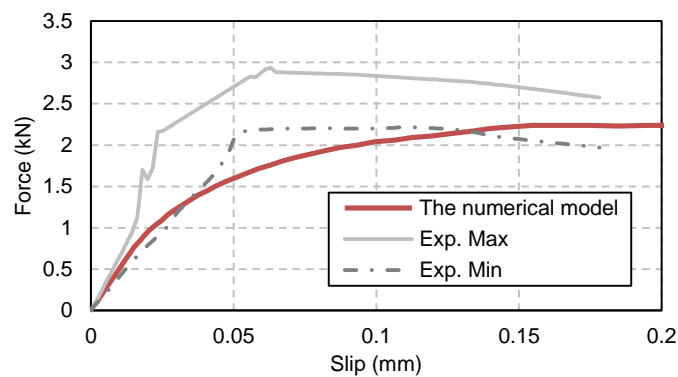
4.3.3. SM bond stress slip law -category 2

The second category of specimens consisted of those cured for one month. As the compressive tests on the samples of the mortar showed the reduction of compressive strength from 13.3 to 12.6 [MPa] respectively for 3 month cured and one month cured samples, it can be concluded that the bond strength also will decrease as a matter of less curing time. Considering this fact and carrying out the sensitivity study for this case as well, the bond stress-slip law for the SM interface in case of simulating the category 2 of specimens is presented in Table 13.

Table 13 - The calibrated bond stress-slip law - SM – C2

SM bond stress-slip law (category 2)

The calibrated variables	
T_m [MPa]	2
T_r [MPa]	0.5
S_0 [mm]	0.0125
S_1 [mm]	0.1
S_u [mm]	0.15
K [N/mm ³]	160

**The resulting bond-slip behaviour of the model**

The obtained numerical result clarifies the appropriateness of the bond stress-slip law calibrated for the SM interface of the category 2 specimens. It provided the same failure mechanism as what was observed in the corresponding experiments together with sufficiently close trend of the global bond-slip response.

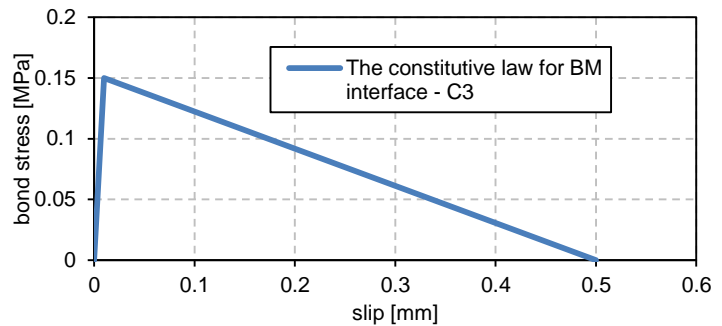
4.3.4. BM bond stress slip law -category 3

In the third category of specimens, the samples have been cured for 1 month and the bricks chosen for being tested have not been sandblasted and they have their original smooth surfaces. This fact led to a different failure mode which was detachment of the mortar from the brick. It is evident the constitutive material law of SM interface is the same as what was introduced in the previous section. All the changes that less curing time would make in the SM constitutive law has been studied through the sensitivity analysis and the calibrated model is introduced which will be used for simulating this category of specimens as well. In this case, it should be considered that what governs the overall behaviour is the bond stress-slip law of the BM interface. The sensitivity analysis on the parameters of this law has led to having the calibrated model as it is presented in Table 14.

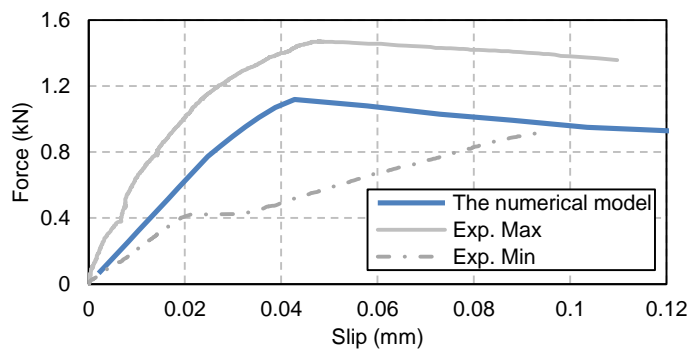
Table 14 - The calibrated bond stress-slip law - BM - C3

BM bond stress-slip law (category 3)

The calibrated variables	
T_{\max} [MPa]	0.15
S_0 [mm]	0.01
S_u [mm]	0.5
K [N/mm ³]	15



The resulting bond-slip behaviour of the model



Regarding the numerical result which has been obtained by applying the bond stress-slip law calibrated for the BM interface for category 3 specimens, it becomes evident that the model is capable of showing the same failure mechanism (de-cohesion of the grout from the brick) as what was observed in experiments as well as providing the global bond-slip behaviour in a good agreement with experimental one.

4.4. Verification of the model assumptions

The assumption of having a linear elastic material constitutive law for the brick, mortar, and the steel cords for this modelling approach can be verified through investigating the stress fields in each material. The maximum principal stress distributions in the materials are controlled in the ultimate stage of the analysis for each category of specimens and have been presented in Table 15, Table 16, and Table 17.

Table 15 - Comparison of the tensile stress (σ_t) and strength (f_t) of the material-C1

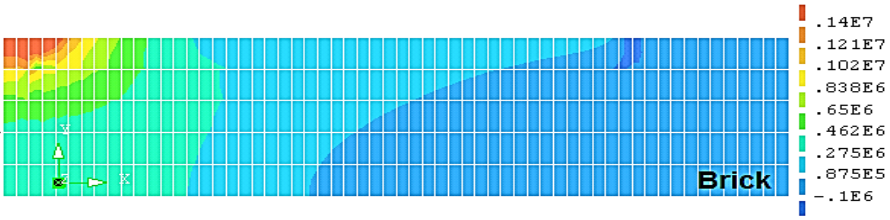
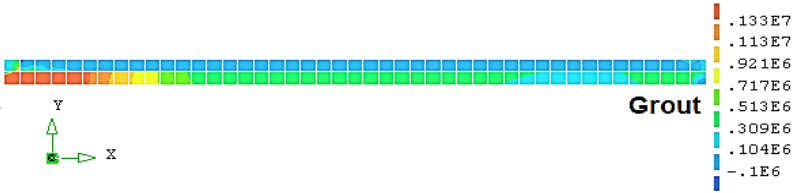

Stress contours in the material	σ_t	f_t
	1.21 [MPa]	1.4 [MPa]
	1.13 [MPa]	1.33 [MPa]
	1160 [MPa]	2820 [MPa]

Table 16 - Comparison of the tensile stress (σ_t) and strength (f_t) of the material-C2

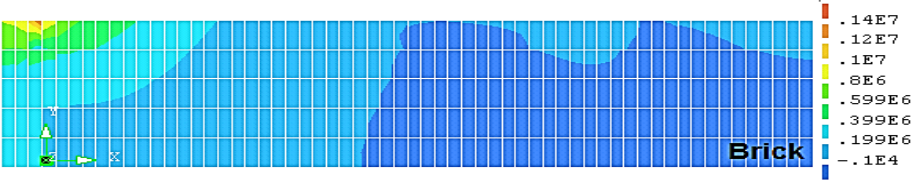
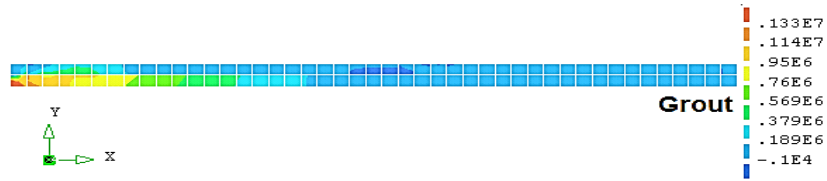

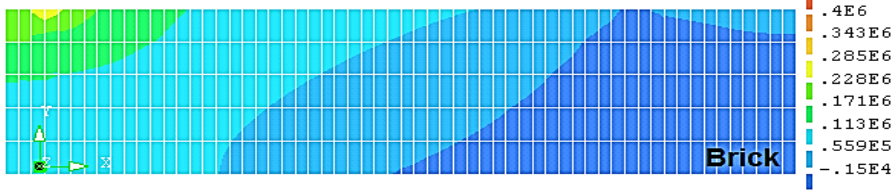
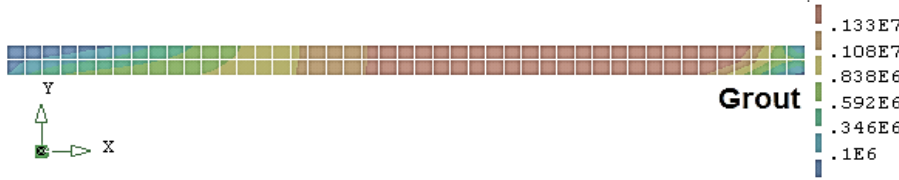
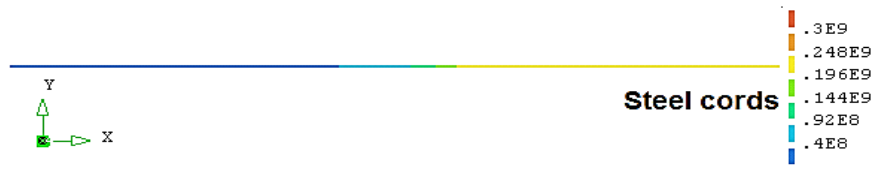
Stress contours in the material	σ_t	f_t
	1.20 [MPa]	1.4 [MPa]
	1.14 [MPa]	1.33 [MPa]
	884 [MPa]	2820 [MPa]

Table 17 - Comparison of the tensile stress (σ_t) and strength (f_t) of the material-C3

Stress contour level in the material	σ_t	f_t
	0.28 [MPa]	1.4 [MPa]
	- [MPa]	1.33 [MPa]
	248 [MPa]	2820 [MPa]

As expected, with the exception of very few localized peak values for the first category in the brick and mortar, the tensile stresses in all the materials are lower than their corresponding strengths. Therefore, the assumption of linear elastic behaviour of materials is confirmed as valid.

Chapter 5

Parametric analysis

Once proved the numerical model capable of simulating different experimental works, it can be used for parametric analysis. A parametric analysis allows obtaining analysis results of multiple cases with the variation of parameters and to understand their relative importance to the structural response. The parameters whose effect of changing will be investigated in this study are those playing important roles in design works. As a matter of designing a strengthening system, it is important to know the qualitative and quantitative effect of composite material properties. As an example, steel sheets are available with different densities and one can choose the best amount by knowing the effect of this parameter, i.e. amount of steel cords on the overall behaviour of the system. Speaking of the quality of the work, it may seem apparent that more amounts of steel cords will result in higher bond strength of the system. However, the quantitative investigations will help to gain more precise knowledge about optimum amounts which will improve the design guidelines as well.

The other parameters are the length of the bond and the thickness of the grout. The effect of these two parameters which basically consider the geometry of the system will help particularly to understand the optimum dimensions of the composite layer. The results of the parametric analysis have been presented in the following sections.

5.1. Width of steel sheets

Different amounts of steel cords have been assumed for the new models. Model P1 has 10 steel cords and model P2 has 6 steel cords; while the original model is consisted of 8 steel cords. In summary, the mechanical properties are the same and only the total cross-section of the truss element as well as the width of the SM interface will increase. The new values of those parameters together with the

consequent result of the analysis have been presented in Table 18. A more visible change of the trend has been illustrated in Figure 21.

Table 18 - The parameter changed in the analysis and the corresponding results.

Model	Width of the SM interface [mm]	Cross section of the Steel cords [mm ²]	Maximum bond resistance of the model [kN]
The original model (8 steel cords)	20.8	4.30	5
P1 (6 steel cords)	15.6	3.23	3.73
P2 (10 steel cords)	26	5.38	6.21

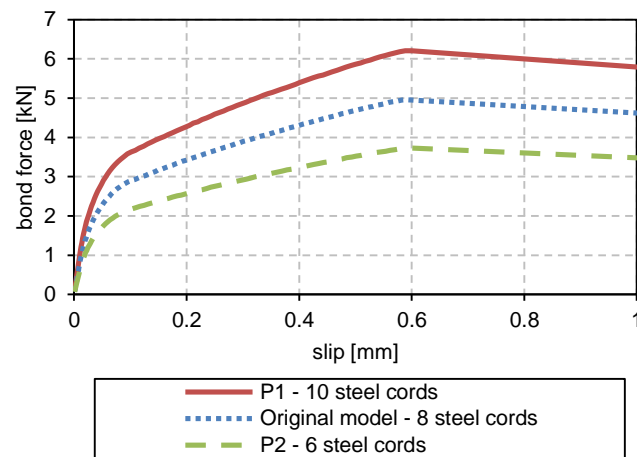


Figure 21 - Results of the parametric analysis on the number of steel cords.

As it was expected, there is a direct relationship between the amount of steel cords used in the reinforcing composite and the bond resistance of the whole system. In model P1 the amount of steel strands has been decreased by 24.8% of the original model in terms of the cross-section of the steel element. The result was 25.4% reduction in the bond resistance of the model (from 5 [kN] to 3.73 [kN]). On the other hand, in model P2 the amount of steel strands has been increased by 25.11% resulting in a rise of 24.2% in the bond resistance. This is due to the type of failure mode occurring. This proportional behaviour will take place until the BM interface becomes nonlinear.

Moreover, it should be mentioned that the maximum bond force is not the only resultant variable which has been changed. The bond force at the elastic limit has decreases by reducing the amount of steel strands. This has to be considered in cases that only elastic regime of the composite system is considered. Finally, it can be concluded that in order to obtain more bond resistance the amount of steel strands can be increased with the direct relation to the desired bond strength. This fact is applicable in case there are no limitations of adding more amount of steel to the system.

5.2. Bonded length

It seems evident that the bond area plays an important role in the composite strengthening techniques. More bond area leads to more bond resistance considering the same characteristics of all material. However, in some cases there are limitations of applying the composite material such as aesthetic aspects, matter of reachability, and etc., a result knowing an optimum bond area will help to design the best possible strengthening system in each particular situation. In this part the effect of having lower bond area has been studied. To be more precise, the width of the bond area has remained fixed and the bond length has been decreased in order to see the consequences of this change. Table 19 represents the changed parameter and the resultant outcome. Figure 22 also shows the outcome in a more visible manner.

Table 19 - The parameter changed in the analysis and the result.

Model	Bond length [mm]	Maximum bond resistance [kN]
The original model	150	5
P3	100	3.93

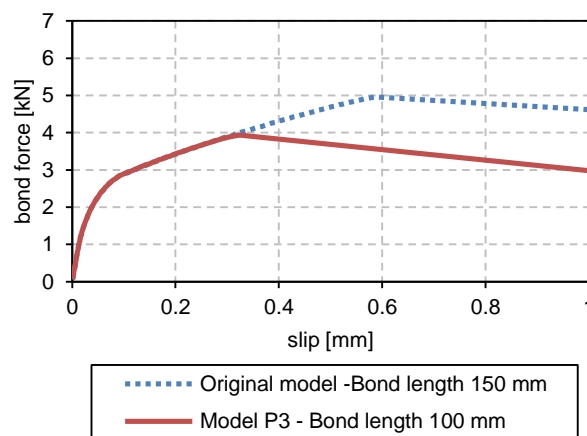


Figure 22 - Results of the parametric analysis on the bond length.

According to the results presented, the expectation of direct relationship between the bond length and the overall bond resistance of the system has been actualized. A 50 [mm] reduction in the bond length (33%), considering the fact that all other parameters have remained the same, caused the 21.07 [kN] of drop in the bond resistance (21%). However, this parameter, contrary to the amount of steel cords, does not affect the bond force of the elastic limit. As a result, in cases where the strengthening systems will work in elastic range the bond length does show significant changes unless the bond resistance drops below the elastic limit.

5.3. Thickness of the grout layer

As it was mentioned before, the grout in this system has the primary responsibility of promoting adhesion of the reinforcing steel to the substrate and later being a cover for steel cords acting as extra protection. This adherent agent plays the important role of transferring stresses through the interfaces between materials; as a result, its physical and mechanical properties should be studied. In this paper it is believed that the mechanical properties of the grout will affect the interfacial behaviour which can be seen in the constitutive laws of the interfaces. In other words, the bond stress-slip law introduced in this paper reflects the particular characteristics of the grout used and another type of grout with different properties will result in a different bond stress-slip law. Therefore, it will be sufficient to study the effect of physical properties of the grout (geometrical aspect) through the parametric analysis.

In this part the thickness of the grout has been increased from 6 [mm] for the original model to 10 [mm] for model P4. The steel cords are placed in the middle and all the other variables are kept fixed. Data regarding this analysis has been presented in Table 20. Figure 23 also shows the resulting bond slip behaviour of the system for the two models: the original model and the model P4.

Table 20 - The parameter changed in the analysis and the result.

Model	Thickness of the grout [mm]	Maximum bond resistance [kN]
The original model	6	5
P4	10	4.96

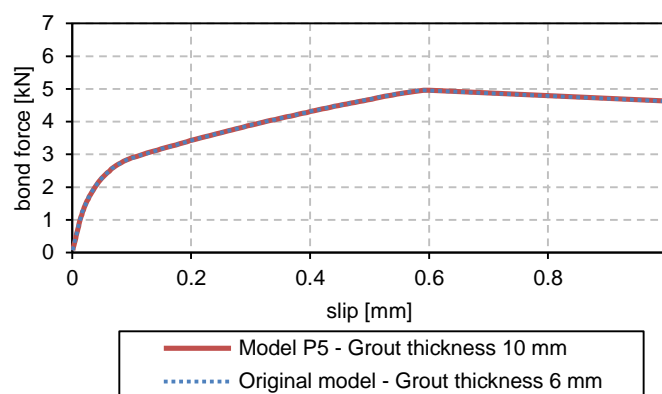
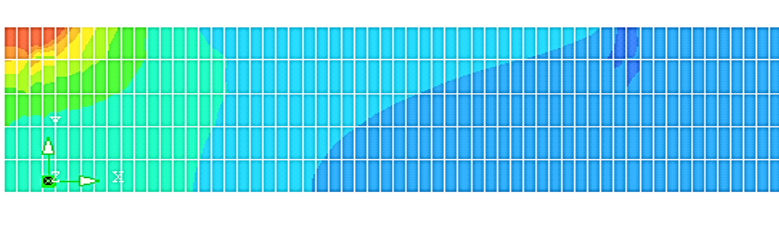
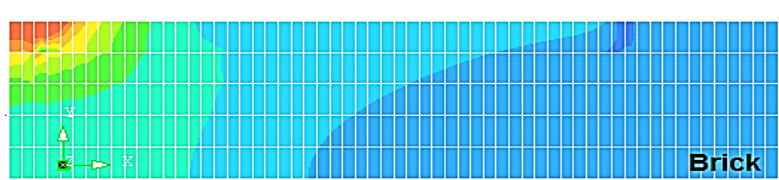

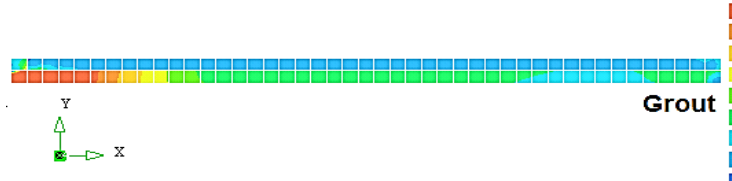


Figure 23 - Results of the parametric analysis on the thickness of the grout.

According to the results, the change in the thickness of the grout does not influence the overall bond slip behaviour of the system. The value of the bond resistance of specimen is almost the same and the resulting graphs of the two models coincide in all ranges. More data has been elicited to investigate the changes more in depth (Table 21).

Table 21 - Stress contours of materials in models P4 and the original model.

Model	Stress contour level in the brick	σ_t (Max)
P4		3.26 [MPa]
Original		3.21 [MPa]
Stress contour level in the mortar		
P4		8.5 [MPa]
Original		7.57 [MPa]

As it can be seen, the localized peak value of the stress has increased. This phenomenon has been also observed by (Wobbe, et al., 2004). The same conclusion can be made that thicker composite layer tend to bring about higher stress concentration at the edges of the composite material. This fact is more apparent in the mortar than in the brick.

5.4. Parameters causing different failure mechanisms to happen

In the last part of the paper, it is worth discussing the capability of the model in representing different failure mechanisms which are probable to happen in different situations for this strengthening technique. The two main failure modes are the slippage of the steel cords from the mortar and de-cohesion of the mortar together with the steel cords from the brick (Figure 11 and Figure 12). These phenomena have been discussed all through the paper; nonetheless, it will be summed up in the following two sections.

In order to understand from the numerical results which of the failure mechanisms have occurred, it is needed to check the slips occurring in each interface separately. This checking was possible through extracting the displacements of four particular nodes, as follows:

- 1 (on the steel element where the steel is attached to the mortar);
- 2 (on the mortar element with the same position of node 1);
- 3 (on the mortar element where the mortar is attached to the brick);
- 4 (on the brick element with the same position as node 3).

The locations of these nodes have been illustrated in Figure 24. The relative displacement of the two nodes 1 and 2 ($\delta_1 - \delta_2$) infers as the slip occurring in the SM interface and the relative displacement of the two nodes of 3 and 4 ($\delta_3 - \delta_4$) refers to slip occurring in the BM interface. Apparently, the interface that has bigger slips will cause the detachment to occur and fails. However, the overall slip presented in all the results before is the relative displacements of the two nodes of 1 and 4 ($\delta_1 - \delta_4$) because this is the value that has been measured in the experiments. This slip value is the sum of slips occurring in both interfaces and regarding the numerical results it is not possible to understand from the final bond slip curve that which kind of failure has occurred. The procedure introduced in this paragraph helps to find out what is the failure mode happening in the numerical model.

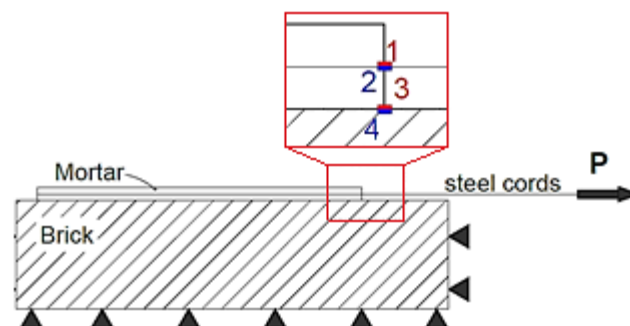


Figure 24 - Location of the nodes whose relative displacement indicated the slip of the model.

Another failure mode which has been observed in rare situations is the tensile failure of the steel cords. This phenomenon will be discussed in the last section in terms of parameters causing this mechanism to happen.

5.4.1. Slippage of the steel cords (SM interface failure)

Regarding all the discussions mentioned previously, the failure mechanism of slippage of the steel cords from the mortar (in other words, failure of the SM interface) happens when the other interface, i.e. BM, is strong enough to transfer the induced stresses from the mortar to the masonry substrates. Using bricks with sandblasted surfaces, like the cases of category 1 and 2 of the experimental work, provides perfect interlocking between the grout and the brick which in terms of strength there will emerge a strong BM interface. In this situation, the applied shear loading will be resisted by the strength of the SM interface and its bond strength governs the failure mechanism. It should be also mentioned that the mechanical properties of materials have considerable roles in the properties of interfaces which is meant to be as indirect effect on the mode of failure.

In addition to parameters mentioned above, the layout of the steel filaments in each steel cord should be considered as well. It is apparent that different ways of twisting the filaments will result in the change in interlocking behaviour between the steel cords and the grout which can be implied as strength of the interface. Stronger is the interface, later will be the slippage which eventually leads to higher bond resistance of the model.

In summary, the behaviour of the SM interface whose failure will cause the mechanism of slippage of the steel cords from the mortar depends on the parameters of:

- Properties of the BM interface (interlocking between the brick surface and the grout).
- The layout of the steel filaments in the steel cords (interlocking between the steel cords and the grout).
- Mechanical properties of the material (affecting the parameters of the constitutive laws of the interfaces)

5.4.2. De-cohesion of the grout from the brick (BM interface failure)

This failure mechanism occurred in the third category of specimens in the experimental tests was simulated with the proposed numerical model introduced in section 4.3.4. As discussed before, a very weak BM interface is the main cause of this failure mechanism. The bricks used in this category had their own original smooth surface which did not provide sufficient interconnection with the grout. The low bond strength and stiffness of the constitutive law obtained for this interface proves this fact. However, a parametric study on the parameters of the constitutive law of the BM interface reveals the information about the influencing variables which can lead to the failure of this interface.

Starting from a perfect bonded BM interface, as it was considered for modelling of the category 1 of the specimens, the variables of the bond stress-slip law of this interface were reduced to see what will be the outcome of the numerical modelling.

In the first step, three different constitutive laws have been assumed for the BM interface and the resulting global behaviour of the model has been observed. The assumed bond stress-slip laws and the corresponding outcomes are presented in Table 22. In order to see which parameters have been assigned for each BM interface Table 23 has been also presented.

Table 22 - Studying the effect of different bond stress-slip laws of BM interface on the global bond-slip behaviour.

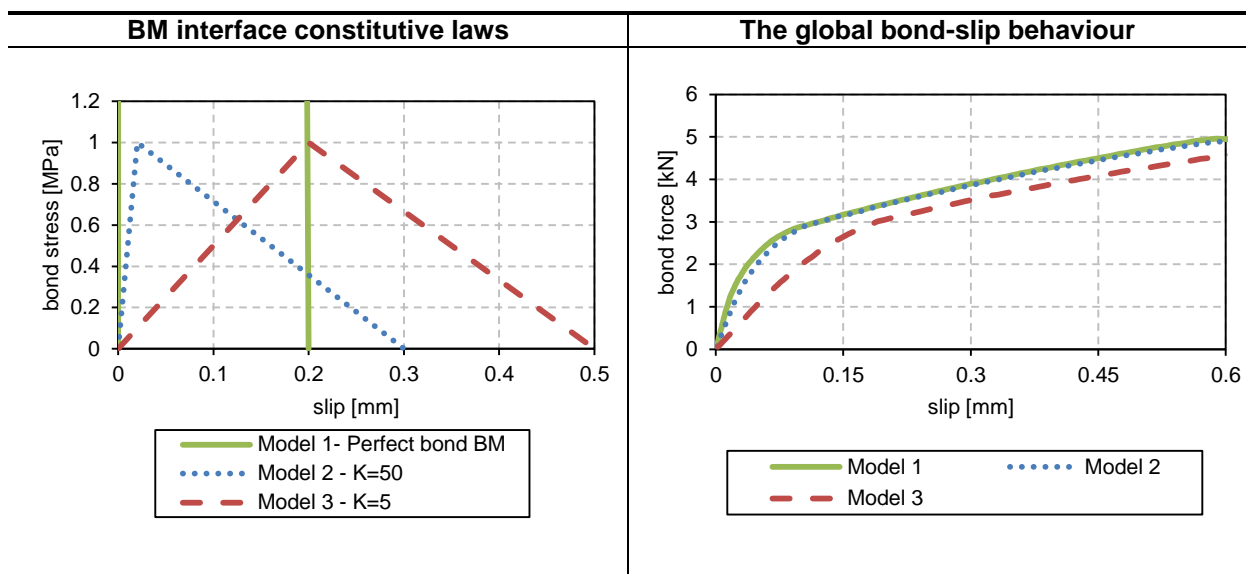


Table 23 - Parameters assigned for each of the BM bond-slip law.

Model 1		Model 2		Model 3	
Bond stress [MPa]	Slip [mm]	Bond stress [MPa]	Slip [mm]	Bond stress [MPa]	Slip [mm]
0	0	0	0	0	0
1000	0.001	1	0.02	1	0.2
0	0.2	0	0.3	0	0.5
K [N/mm ³]	1.E+06	K [N/mm ³]	50	K [N/mm ³]	5

As it can be seen the three models have stiffness and bond strength values differing in the vast range from 1E6 [N/mm³] and 1000 [MPa] to 5 [N/mm³] and 1 [MPa], respectively, but the global result do not show noticeable differences. In the results of the third model which has the stiffness of 5 [N/mm³], can be seen a slight reduction in the stiffness and bond force values of the global behaviour (the maximum bond resistance has changed from 5 to 4.89 [kN] in model 3). However, in the way it is explained in the beginning of the chapter, it was found out that all the failure modes were the slippage of the steel

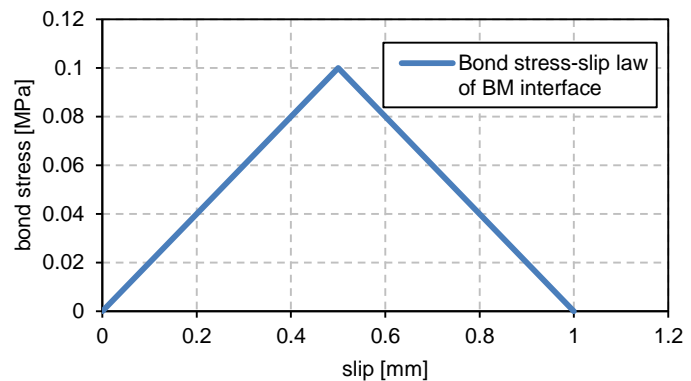
cords from the mortar. This fact leads to the conclusion that even a very weak BM interface with the bond strength of 1 [MPa] and stiffness of 5 [N/mm³] does not fail before the SM interface.

In the second step, the parameters of the BM interface bond stress-slip law were reduced more to see when the failure mode will be the detachment of the mortar from the brick. The following bond stress-slip law introduced in Table 24 for the BM interface is the answer of the asked situation.

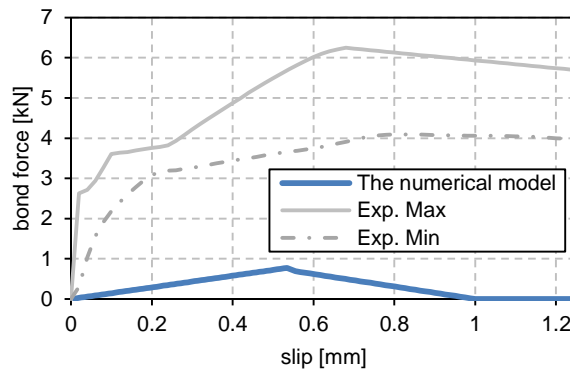
Table 24 - BM bond stress-slip law which results in the failure mode of de-cohesion of the mortar from the brick.

BM bond stress-slip law (category 3)

The calibrated variables	
T_{\max} [MPa]	0.1
S_0 [mm]	0.5
S_u [mm]	1
K [N/mm ³]	0.2



The resulting bond-slip behaviour of the model



According to the results, assuming the bond strength of the BM interface as low as 0.5 [MPa] together with a very low stiffness value of 0.2 [N/mm³] causes the detachment of the mortar from the brick to precede the slippage of the steel cords from the mortar.

It is worth restating that from the bond force-slip graph presented (the global bond slip behaviour) it is not possible to understand which failure mechanism has occurred. The understanding of this fact is possible through checking the slip occurred in each interface separately (as explained in the beginning of this chapter). In all the cases that the bond force-slip graph (the global bond slip behaviour) was presented, this matter was checked and the failure mode was reported. The interesting fact is that in

all the cases that the failure mode is the failure of the BM interface the bond resistance cannot increase to a noticeable value. In other words, having a bond resistance of about 5 [kN] requires a strong BM interface which will never fail, otherwise, it has been observed that the bond resistance cannot reach the value of 5 [kN].

5.4.3. Tensile failure of the steel cords

The maximum normal stresses in the steel element of the model relating to the category 1 of the specimens have been captured in different load steps and presented in Figure 25.

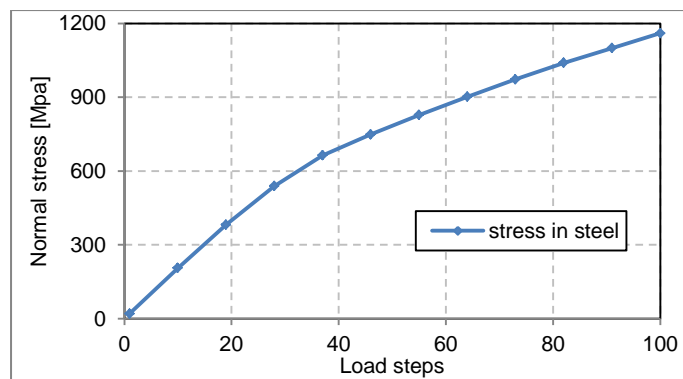


Figure 25 - Normal stresses in steel cords in different load steps.

As it can be seen, in this model the maximum normal stress induced in the steel cords in the ultimate step of loading is still much lower than their tensile strengths ($\sigma_t=1160$ [MPa] < $f_t=2820$ [MPa]). Apparently, the tensile failure mode is improbable in this case.

However, using different kinds of steel cords with lower values of tensile strengths will result in occurrence of this failure mechanism. Capturing the corresponding bond force and slip values to specific steel stress values; the graph presented in Figure 26 will be obtained. This figure indicates failure mechanisms of the model in case of using steel cords with the same geometrical and physical characteristics but lower tensile strengths. Table 25 represents the exact data on which Figure 26 is based on.

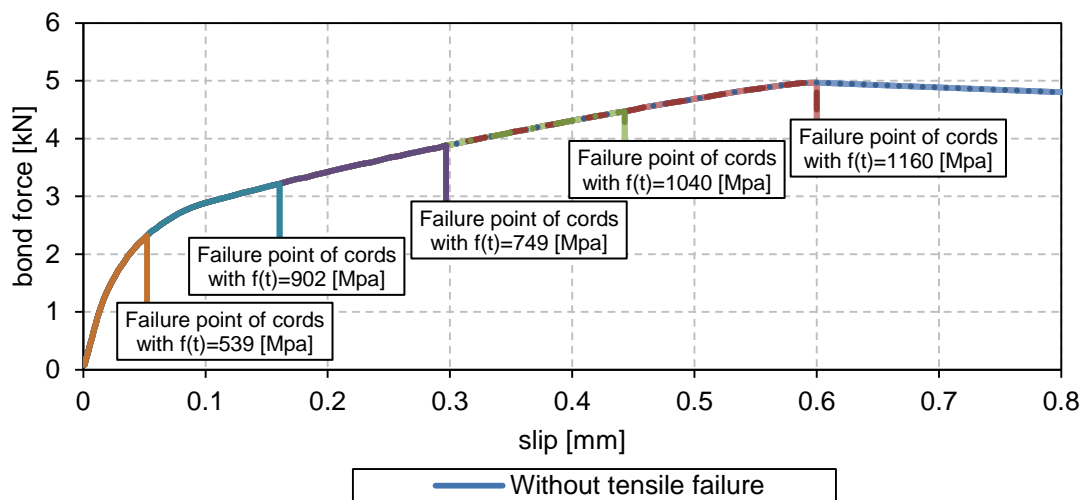


Figure 26 - Tensile failure of different types of steel cords in different load steps.

Table 25 - Values of stresses in steel cords and corresponding bond forces and slips.

Load step	10	19	28	37	46	55	64	73	82	91	100
Stress in steel [MPa]	206	382	539	664	749	828	902	973	1040	1100	1160
Bond force [MPa]	0.88	1.64	2.32	2.86	3.22	3.56	3.88	4.18	4.47	4.75	5
Slip [mm]	0.01	0.026	0.052	0.095	0.161	0.228	0.297	0.369	0.443	0.518	0.600

According to the data presented (Figure 26 and Table 25), it can be seen that by using steel cords with lower tensile strengths, the failure of the model precedes, besides, bond resistance decreases. Together with the fact that in this case less than half of the tensile capacity of the steel cords has been used, it can be concluded that according to the desired amount of increase in the bond resistance of the element a special type of steel sheet with optimum tensile strength can be chosen. It should be also kept in mind that the other failure mechanisms should not fall behind the tensile failure by defining proper constitutive laws for BM and SM interfaces which are influenced by several factors as discussed in the two previous sections. That is, by changing the steel cords their arrangements and other properties which affect the characteristics of BM and SM interfaces may also change and in this case the new model should be calibrated and the occurrence of the type of the failure mechanism should be checked. Then, the decision on the best choice for the type of steel cords can be made.

Chapter 6

Conclusion and further remarks

6.1. Main conclusions

Aiming at understanding the bond behaviour in SRG-strengthened masonry elements, a numerical model is developed which is able to simulate the performance of this strengthening technique. Regarding experiments carried out at University of Minho on three different categories of specimens and the results obtained, it was possible to gain the knowledge of the overall behaviour of the system as well as to learn possible failure mechanisms which occur in different cases. It is worth mentioning that it is the first time that the specific characteristics of interfacial behaviours are investigated separately and the global behaviour has been analysed in a micro scale as specific as to identify what are the conditions for each failure mechanism to happen. The peculiarity of the research was to find out the constitutive laws of the interfaces whose nonlinear behaviours would define the global bond-slip response of the system. Without measurements on the local bond stress-slip relationships of the interfaces, it was possible to justify the missing data through a reverse analysis. The ability of the proposed model to be justified for different cases proves the reliability of this approach.

As the first conclusion, it can be said that the proposed numerical model is capable of representing different failure modes with the prescribed conditions which are basically unknown. Discovering those conditions implies for having specific behaviour for the constituents which bring about understanding the role of each component. The global response is stated as bond-slip behaviour and it turned out to be dependent on the local bond stress-slip behaviour of interfaces. As it is predefined, the term bond accounts for the shear stress transfer between two different materials which are in contact with each other through an interface. The composite strengthening system whose bond characteristics are being investigated comprises of two interfaces: one representing the interaction between the grout and the brick and the other one indicating for the interconnection of the steel cords and the surrounding grout. The analysis of the numerical results evidenced that with having enough mechanical interlock in the BM (brick-mortar) interface, the failure mode of de-cohesion of the grout from the masonry substrate

will be faded. Sandblasting the surfaces of the bricks is a way of producing such interfacial mechanical interlock. As stated in the literature, some additives to the grout could also result in a similar outcome. Speaking of the quantities, the stiffness of a BM interface leading to the global failure mode of detachment of the grout from the brick, can be as small as $0.2 \text{ [N/mm}^3\text{]}$ with the assumed interfacial bond strength of 1 [MPa] . Otherwise, having a stiffness of 50 or $1\text{E}6 \text{ [N/mm}^3\text{]}$ will result in the same global bond-slip behaviour which will be only influenced by characteristics of the other interface named SM (steel-mortar interface). This situation has been referred to as a perfectly bonded BM interface in this paper.

In continuation of the aforementioned condition for BM interface, it was concluded that the characteristics of the bond stress-slip law of the SM interface are effective when the failure mechanism happening is the slippage of the steel cords from the grout. The calibration of the model could provide the shear stiffness, bond strength, residual bond stress, and other unknown parameters of the interfacial bond stress-slip law. The numerical results obtained which could both represent the global bond slip behaviour with very good agreement as well as reproduce the failures observed in experiments confirmed the accuracy of that the basic assumptions made in this approach. The overall shape of the local bond stress-slip relationships of the interfaces was a matter of question which could be adopted from a relevant situation. Considering the materials (brick, mortar, and steel cords) constitutive law as linear and concentrating all the nonlinearities in the behaviour of the two interfaces were the other assumption which could be verified through checking the stress state of the material in different stages of loading. Another failure mechanism which is rarely probable to occur, i.e. tensile failure of the steel cords, has been discussed and the conditions for such phenomenon to be reproduced were presented.

Being confident on the accuracy of the proposed model, parametric analysis was carried out. The parameters being effective in designing procedure were considered to be investigated. The results let to such conclusions to be drawn: the width of the steel cords used in the SRG strengthening system has a direct influence on the bond resistance, the bond length of composite layer has also similar effect but not in the hardening part of the global bond slip-behaviour in case of comparing to the parameter of width of the steel cords, and finally the thickness of the grout showed negative influence since the thicker grout resulted in the increase of the stress concentration at the edges of the composite layer.

As the final conclusion, it can be said that even in the cases that it is not possible to measure or gather all the required data, there will be innovative approaches to solve the problem.

6.2. Remarks for further investigations

Recommendations for subsequent investigations on the present research topic can be classified in two groups. The first regards the numerical point of view for which there is the possibility to adopt more complexities in case of having more comprehensive knowledge. The complexities can be related to the constitutive laws assumed for both material and interfaces. The only matter to be considered about the linearity of the material is the presence of the localized peak stress values in the mortar and brick which it will not seem unreasonable to be considered otherwise if the facilities for such a more complicated case are provided. Modelling of the masonry prisms in order to assess the possible influence of mortar joints is also another remark. The bond stress-slip relationship defined for the SM interface was proved to be a good representative of the actual case but for the BM interface more data was missing. With regard to the experimental data available, the most possible facts were checked in the numerical modelling. Consequently, the second group can be classified as further investigations on the experimental point of view. Carrying out more research on the innovative ways of measuring local strains at the interfaces is one of the suggestions. Measuring the global slip value in a different way also will result in finding out more about the individual characteristics of the interfaces.

References

Barton B. [et al.] Characterization of reinforced concrete beams strengthened by steel reinforced polymer and grout (SRP and SRG) composites [Journal] // Materials science and engineering. - 2005.

Borri A., Castori G. and Corradi M. Shear behavior of masonry panels strengthened by high strength steel cords [Journal] // Elsevier Construction and Building Materials. - 2011.

Borri Antonio [et al.] Strengthening of Brick Masonry Arches with Externally Bonded Steel Reinforced Composites [Conference] // CCENG-45. - 2009.

Borri Antonio, Castori Giulio and Grazini Andrea Performance of masonry elements strengthened with steel reinforced grout [Conference] // FRPRCS. - Patras, Greece : [s.n.], 2007.

Chajes M.J. [et al.] Bond and force transfer of composite material plates bonded to concrete [Journal]. - [s.l.] : ACI structural journal, 1996. - 2 : Vols. 93,.

CNR-DT200 Guide for the design and construction of externally bonded FRP systems for strengthening existing structures. [Book Section]. - 2012.

De Lorenzis Laura, Miller Brian and Nanni Antonio Bond of FRP laminates to concrete [Journal]. - [s.l.] : ACI Materials Journal, 2001. - No. 3 : Vol. 98.

Dhanasekar M. and Haider W. Explicit finite element analysis of lightly reinforced masonry shear walls [Journal] // Computers and Structures. - 2008. - pp. 15-26.

DIANA Displacement analysis finite element software.. - Delft, The Netherlands : TNO building division, 2009. - Vol. 9.4..

fib Bulletin No.55 Model Code 2010 - First complete draft, Volume 1 [Report]. - 2010.

Ghiassi B. [et al.] Meso-scale three-dimensional modeling of bond in FRP-strengthened masonry [Conference] // ECCOMAS Young investigators conference. - Aveiro, Portugal : [s.n.], 2012.

Ghiassi Bahman [et al.] Numerical analysis of bond behavior between masonry bricks and composite materials [Journal] // Elsevier Engineering Structures. - [s.l.] : Engineering structures, 2012.

Grande Ernesto, Imbimbo Maura and Sacco Elio Modeling and numerical analysis of the bond behavior of masonry elements strengthened with SRP/SGR [Journal] // Composites: Part B. - 2013.

Hollaway L.C. A review of the present and future utilisation of FRP composites in the civil infrastructure with reference to their important in-service properties [Journal]. - [s.l.] : Construction and building materials, 2010.

Huang X. [et al.] Properties and potential for application of steel reinforced polymer and steel reinforced grout composites [Journal]. - [s.l.] : Composites: Part B engineering, 2005.

Lourenço Paulo B Computations on historic masonry structures [Book Section] // Progress in structural engineering and material. - 2002. - Vol. 4.

Matana M. [et al.] Bond performance of steel reinforced polymer and steel reinforced grout [Conference] // International Symposium on Bond Behaviour of FRP in Structures (BBFS). - 2005.

Morbin Antonio Strengthening of masonry elements with FRP composites [Report]. - [s.l.] : Center for infrastructure engineering studies, University of Missouri-Rolla, 2002.

Najm H. and Naaman A. E. Bond-Slip Mechanisms of Steel Fibers in Concrete [Journal] // ACI materials journal. - 1991.

Oliveira Daniel V. Experimental and numerical analysis of blocky masonry structures under cyclic loading [Report]. - [s.l.] : Ph.D. thesis, University of Minho, 2003.

PLEȘU RALUCA [et al.] Strengthening and rehabilitation conventional methods for masonry structures [Conference] // BULETINUL INSTITUTULUI POLITEHNIC DIN IAȘI. - [s.l.] : Universitatea Tehnică „Gheorghe Asachi” din Iași, 2011.

Setunge Sujeeva [et al.] Review of strengthening techniques using externally bonded FRP composites [Report]. - [s.l.] : CRC Construction Innovation, 2002.

Tomazevic M., Lutman M. and Petrovic L. In plane behaviour of reinforced masonry walls subjected to cyclic lateral loads [Report]. - Ljubljana, Slovenia : [s.n.], 1993.

Valluzzi M.R. [et al.] Round robin test for composite-to-brick shear bond characterization [Journal]. - [s.l.] : Materials and structures , 2012.

Wobbe E. [et al.] Flexural capacity of RC beams externally bonded with SRP and SRG [Conference]. - 2004.